Locus coeruleus activation 'resets' hippocampal event representations and separates adjacent memories

David Clewett[1*], Ringo Huang[1], & Lila Davachi[2,3]

[1]Department of Psychology, UCLA, USA
[2]Department of Psychology, Columbia University, USA
[3]Nathan Kline Institute, Orangeburg, New York, USA

*To whom correspondence should be addressed:

Department of Psychology
University of California, Los Angeles
5558 Pritzker Hall
Los Angeles, CA 90095
Email: david.clewett@psych.ucla.edu

Keywords: episodic memory, arousal, pupil, time, norepinephrine, dopamine, event boundary

Author Contributions: D.C. and L.D. conceptualized and designed the experiment; D.C. collected data; D.C., and R.H. analyzed the data; D.C and L.D. wrote the manuscript. R.H. helped revised the original manuscript.

Acknowledgements: This project was funded by federal NIH grant R01 MH074692 to L.D. and by fellowships on federal NIH grant F32 MH114536 to D.C. We thank Ziyuan Chen for her assistance with locus coeruleus tracing. We thank Alexandra Cohen and Erin Morrow for helpful feedback on earlier versions of this manuscript. Additionally, we thank Nina Rouhani for stimulating conversations about these ideas. We dedicate this paper to Dr. Carolyn Harley, a treasured colleague and pioneer of locus coeruleus and memory research. The significant impact of her work is only outmatched by her generosity of spirit, kindness, and child-like enthusiasm for neuroscience research.

Abstract

Memories reflect the ebb and flow of experiences, capturing unique and meaningful events from our lives. Using a combination of functional magnetic resonance imaging (fMRI), neuromelanin imaging, and pupillometry, we show that arousal and locus coeruleus (LC) activation transform otherwise continuous experiences into distinct episodic memories. As sequences unfold, encountering a context shift, or event boundary, triggers arousal and LC processes that predict later memory separation. Boundaries furthermore promote temporal pattern separation within left hippocampal dentate gyrus, which correlates with heightened LC responses to those same transition points. We also find that a neurochemical index of prolonged LC activation correlates with diminished arousal responses at boundaries, suggesting a connection between elevated LC output and impaired event processing. These findings align with the idea that arousal processes initiate a neural and memory 'reset' in response to significant changes, constructing the very episodes that define everyday memory.

Introduction

As time passes, we are exposed to a continuous stream of information. To make sense of it all, individuals tend to group similar information into distinct mental 'episodes' based on context, like place or time[1]. For instance, being in your kitchen helps create a unique memory of "breakfast" by linking various details like eggs, the table, and time of day together. Conversely, transitioning to a new context or situation, like leaving home for work, facilitates perception of a new event[1,2]. Memory formation therefore involves a delicate balance between integrating continuous information and segmenting distinct episodes in perception and memory, often triggered by context shifts that act as event boundaries[3–5]. A wealth of research supports this idea that contextual stability facilitates temporal integration of elements into coherent memories. Further, empirical studies demonstrate that a wide variety context changes, such as shifts in space[6], emotion[7], goals[8–13], or perceptual features[14–16], lead to the separation of adjacent memories, as indexed by disruptions in binding and remembering sequential information. While these behavioral effects are robust and replicable, little is known about the mechanisms triggered at boundaries that adaptively segment and encode unique new memories.

It is widely recognized that the hippocampus plays a critical role in binding sequential or temporal associations that are essential to episodic memory[4,17–22]. Research indicates that as time unfolds, a constant push-and-pull process between hippocampal encoding and retrieval mechanisms helps promote the storage of distinct memories. When encountering new information, hippocampal operations must determine whether this information is stored as a distinct memory trace (i.e., requiring 'pattern separation'[23,24]) or incorporated into existing memory representations (i.e., requiring 'pattern completion'[25,26]). Importantly, hippocampal processes also appear to be sensitive to event structure, with boundaries eliciting univariate hippocampal activation patterns that relate to successful encoding and consolidation of recent events[4,27–32]. Focusing on hippocampal activation at event boundaries, however, has led researchers to overlook a fundamental question: what signals tip the balance between hippocampal separation and integration processes?

One possibility is that the locus coeruleus (LC), the primary supplier of norepinephrine (NE) to the brain, is the origin and substrate of this neural signal, serving to 'reset' hippocampal and memory representations during context shifts. Through its widespread projections, the LC facilitates arousal, attention, and memory processes during salient occurrences[33–36]. LC neuronal inputs are particularly dense to the dentate gyrus (DG) subfield of the hippocampus, a region implicated in pattern separation[24]. This specialized anatomy provides a pathway through which noradrenergic activity could amplify memory separation at boundaries and help to disambiguate representations of temporally adjacent contexts[37–39]. Functionally, the LC-NE system is ideally suited for signaling and mediating the impact of event boundaries on memory. Phasic LC responses signal contextual novelty and aid in encoding new memories[35,40–42]. When expectations about unfolding experiences are violated, phasic LC responses help signal prediction errors that rapidly update mental models of what is happening[46–4.43]. The resulting global release of NE is thought to initiate a 'network reset', whereby functional brain networks are reorganized to prioritize processing new information[44,45]. In everyday life, event boundaries punctuate and signal critical moments of change in the world. Consequently, our ability to understand unfolding experiences may depend on a rapid and behaviorally relevant updating signal from the LC when something surprising, unexpected, or important occurs.

Studies examining pupil dilation, a putative index of LC activity[46–51], provide initial support for the idea that the noradrenergic system helps structure memory. We have previously demonstrated that event boundaries reliably elicit pupil dilation, a physiological index of arousal[16]. Moreover, distinct temporal components of these pupil dilations also relate to behavioral correlates of event segmentation, including subjective time dilation and reduced temporal order memory for information spanning those transitions[16]. These correlational findings are also corroborated by studies that manipulate arousal states more directly. For example, highly arousing emotional sounds elicit event segmentation during sequence encoding, as indexed by impaired temporal order memory for information spanning those negative stimuli[7]. Converging findings from computational and empirical studies furthermore demonstrate that prediction error-related arousal alters the temporal organization of events in memory[52]. However, whether these connections between arousal and memory organization reflect changes in LC-NE activation remains unclear.

Here, we combined high-resolution functional magnetic resonance imaging (fMRI) and pupil dilation, a biomarker of arousal, to measure human brain activity during the well-validated Ezzyat-Dubrow-Davachi (EDD) Paradigm[16,53]. Our primary goals were to investigate relationships between arousal, LC activation, and temporal memory measures of event segmentation at boundaries. As before, pupil size was measured continuously to examine if dynamic fluctuations in arousal track event structure and encoding processes[16]. Using fMRI pattern similarity analyses, we also investigated if boundaries reduce the stability of DG neural patterns across time, indexing pattern separation of distinct mental contexts when it is warranted. We then examined if neural pattern differentiation across event boundaries was related to a transient increase in LC activation. Finally, taking an individual differences approach, we also examined whether a structural trait-like measure of tonic, or sustained, LC activation relates to neurophysiological signatures of event segmentation. Specialized neuroimaging sequences now enable the precise localization of the LC through their sensitivity to neuromelanin, a pigmented neurochemical that is a byproduct of NE metabolism[54–56]. In young adults, it has been speculated that higher LC signal intensity may capture repeated stress-related activation of the noradrenergic system. For example, LC signal intensity is higher in individuals with PTSD compared to those without PTSD[57], and relates to heart-related measures of elevated sympathetic nervous system activity[58,59]. Our goal, therefore, was to see if this indirect measure of tonic LC activity relates to event processing.

Our findings support the idea that noradrenergic mechanisms contribute to the adaptive structuring of memory. First, lending reliability to our prior findings, we replicate the established behavioral findings showing that context shifts elicit behavioral memory separation and pupil-linked arousal[16]. We also find evidence for the critical missing link between LC activation and memory separation: boundary-induced LC activation selectively correlates with order memory impairments across boundaries and not within events. Interestingly, engagement of the LC at boundaries also specifically relates to a temporal feature of pupil dilation thought to regulated by sympathetic nervous system pathways[60]. We furthermore find that boundaries result in a change in neural patterns between event-spanning items in left DG, with DG pattern differentiation being predicted by heighted LC activation. This finding aligns with the notion of an LC-mediated ‘reset’ signal that functionally configures hippocampal networks to represent contextually distinct events. Finally, we demonstrate that higher LC neuromelanin signal intensity is associated with diminished boundary-induced pupil dilations during event encoding, pointing to a potential connection between chronic LC activation and impaired event processing.

Behavioral Results

Event boundaries increase response times and induce event segmentation effects in long-term memory. In the current event sequence paradigm, participants studied lists of neutral objects while listening to simple tones played in their left or right ear (**Figure 1A**)[16]. Stability and change in the surrounding auditory context were used to create the perception of stable auditory 'events' and 'event boundaries', respectively. Eight pure tones were repeated in the same ear to create a sense of contextual stability. However, after 8 successive items, the tone switched to the other ear and changed in pitch to elicit perception of an auditory context shift, or event boundary. The new tone/ear then remained the same for the next 8 items before switching back again and so on.

To examine how these boundaries influenced attention during encoding (**Figure 1A**), we compared response times to boundary items and same-context items for the size judgements participants made for each object. As expected, participants were slower at judging objects that appeared immediately after a tone switch (*M* = 1178ms, *SD* = 274) compared to items that appeared after a repeated, same-context tone (*M* = 1114ms, *SD* = 286; ß = 0.12, p < .001, 95% CI [0.08, 0.15]; **Figure 1B**). This response-time slowing effect most likely reflects a cognitive switching cost rather than a motor switching cost, as participants had ample time to switch hands during the tone cues (range: 1.5-3.5 seconds from tone to response).

Turning to the long-term consequences of this enhanced local boundary processing, we examined if tone switches led to more expanded estimates of temporal distance and impairments in temporal order memory between item pairs from the prior sequences – two behavioral measures of event segmentation[4]. Here, we specifically focused on temporal order memory effects, given recent predictions that noradrenergic system activation primarily elicits segmentation by disrupting temporal binding processes[61]. Replicating prior work with the EDD paradigm, we found that temporal order memory was significantly impaired for boundary-spanning item pairs relative to same-context item pairs (ß = -0.14, p < .001, 95% CI [-0.21, -0.07], odds ratio = 0.87; **Figure 1C**).

Interestingly, we also found a relationship between these behavioral measures, with increased attention at boundaries relating to subsequent impairments in temporal order memory. This trade-off effect suggests that greater local processing at an event transition occurs at the expense of maintaining temporal encoding processes across time[15]. We report these results below (see section titled "**Individual Differences Correlations between Arousal, LC Measures, and Behavior").** In summary, our behavioral results accord with the idea that boundaries elicit attention and support the temporal organization of events in long-term memory.

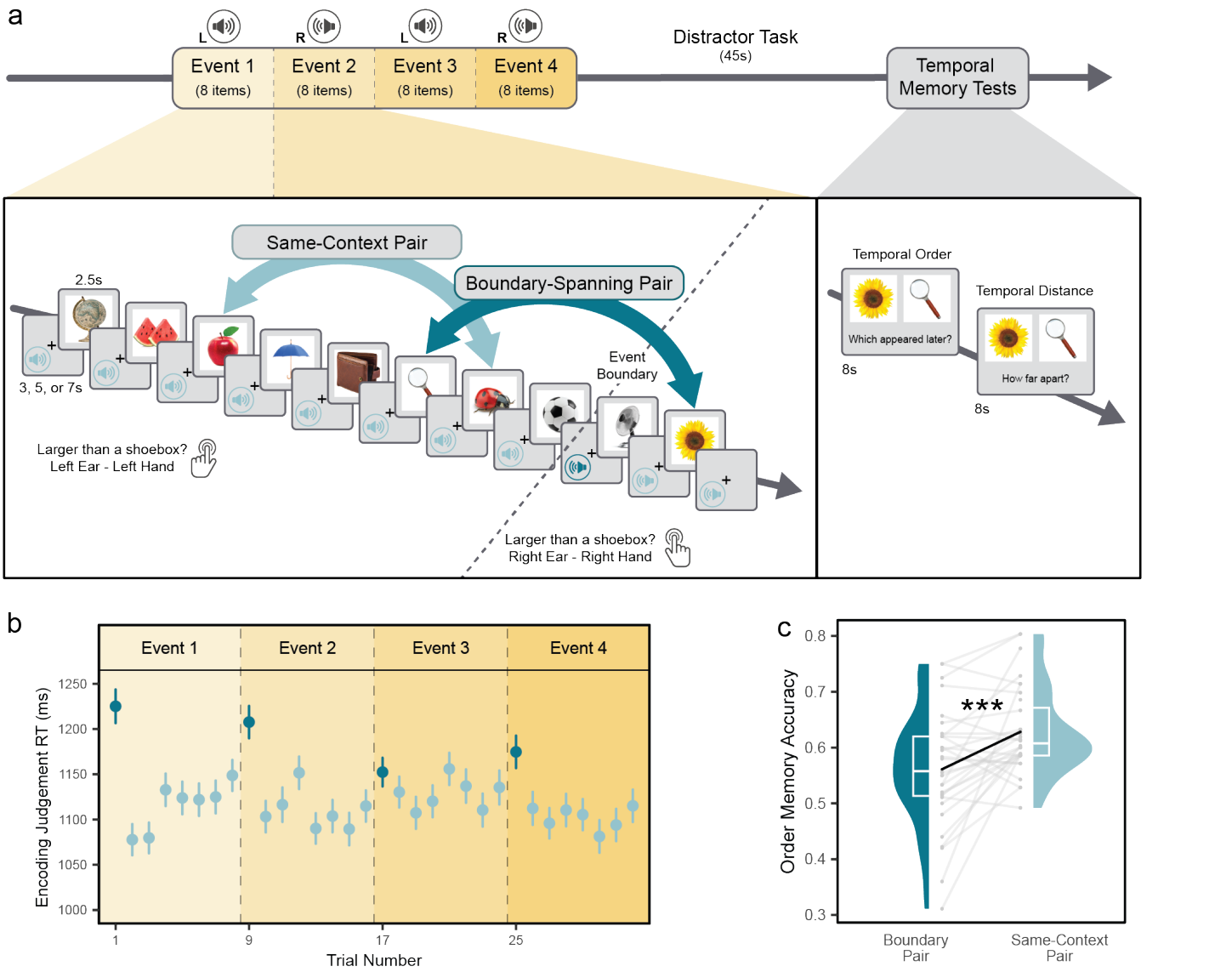

Figure 1. Auditory event boundaries elicit increased attention and the segmentation of distinct events in memory. (A) In the event sequence task, participants studied slideshows of 32 neutral object images. Prior to each image, participants heard a pure tone in either their left or right ear, which signaled which hand they should use to judge the size of each object. After 8 successive items in each list, the tone switched to the other ear, changed in frequency, and then repeated for the next 8 items and so on. Thus, repeated tones created a stable auditory event, whereas tone switches created 'event boundaries' that divided an otherwise continuous sequence into four events. Following each list, participants performed two temporal memory tests used to operationalize event segmentation: temporal order memory and temporal distance ratings. (B) Responses times (RTs) for the object judgements plotted by item position in the 32-item list. Dark blue colors indicate boundary items, or objects following a tone switch. Light blue items indicate objects that immediately followed a same-context, or repeated tone, within an 8-item auditory event. Dots represent mean response times at a given item position and vertical solid bars represent standard errors of the mean (s.e.m.). (C) Event boundaries impaired later temporal order memory for item pairs that had spanned an event boundary compared to pairs encountered within the same auditory context. Colored boxplots represent 25th–75th percentiles of the data, the center line the median, and the error bars the s.e.m. Individual dots represent individual participants (n = 32). Note that statistical results reflect results of a logistic mixed effects model, and this figure is meant to illustrate data distributions. ***p < .001.

Univariate LC fMRI Results

LC BOLD activation at boundaries relates to impairments in temporal order memory, a behavioral index of memory separation. Turning to our key hypotheses, we examine if LC activation at event boundaries (i.e., tone switches) relates to later memory separation. Overall, there was no significant modulation of LC BOLD activation either by boundary tones (*M* = 2.06, *SD* = 715.47; t(862) = .08, p = .93, 95% CI [-45.68, 49.81]) or by same-context tones (t(8387) = 0.13, p = .89, 95% CI [-14.68, 16.83]) relative to baseline (**Figure 2A**). We also did not find a significant difference in LC activation between conditions (*M* = 1.14, *SD* = 663.87; ß = 6.93e-04, p = .97, 95% CI [-0.03, 0.04]), suggesting that, on average, encountering a boundary does not always elicit a strong LC response.

Although boundaries did not reliably activate the LC across the task, we were most interested in seeing whether trial-level engagement of the LC was related to the temporal order memory impairments observed at boundaries. Consistent with this core prediction, logistic mixed effects modeling revealed a significant condition-related interaction effect of LC activation on temporal order memory, such that tone-evoked LC responses were significantly more associated with order memory impairments on boundary trials compared to same-context trials (ß = -0.11, p = .002, 95% CI [-0.18, -0.04], odds ratio = 0.90, **Figure 2B**).

When examining the two conditions separately, we found that this interaction effect was driven by trial-level boundary-induced LC activation relating to larger impairments in temporal order memory (ß = -0.18, p < .001, 95% CI [-0.29, -0.08], odds ratio = 0.83; **Figure 2B**). This LC-memory relationship was not seen for same-context item pairs (ß = 0.05, p = 0.33, 95% CI [-0.05, 0.14], odds ratio = 1.05, **Figure 2B**). Thus, these results show that activation of the noradrenergic system at boundaries relates to disruptions in the sequential integration of items in long-term memory.

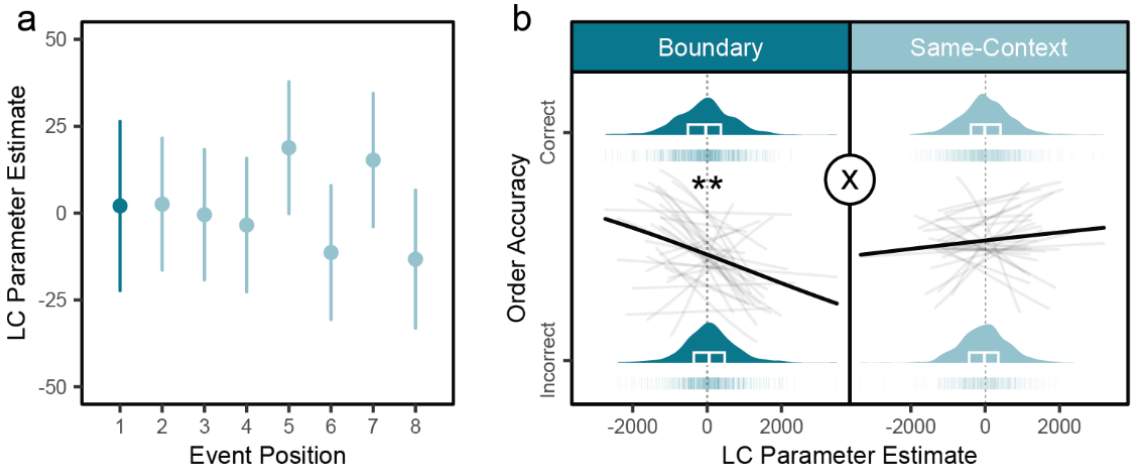

Figure 2. Locus coeruleus (LC) activation at event boundaries relates to impaired temporal order memory, an index of behavioral memory separation. (A) Mean LC parameter estimates to each tone during encoding plotted as a function of item position within the 8-item auditory events. Boundary-related LC responses (item position #1 within an event) are displayed in dark blue, whereas repeated tone-evoked LC responses (item positions #2-8 within an event) are displayed in light blue. Vertical bars represent s.e.m. (B) Trial-level logistic regression between tone-evoked univariate LC activation and temporal order memory

accuracy, separated by condition (item pair type). Results show that tone-evoked LC activation was selectively correlated with order memory impairments for boundary-spanning item pairs but not same-context pairs. Dark, bold lines represent the average regression slope across all participants. Light grey lines represent regression slopes for each participant from the logistic regression. Plots display density distributions and colored boxplots represent 25th–75th percentiles of the data, the center line the median, and the error bars the s.e.m. The data includes *n* = 32 participants. **p < .01 main effect for boundary trials. The "X" symbol indicates significant LC-by-condition interaction effect at p < .001.

Hippocampal Pattern Similarity fMRI Analyses

Event boundaries promote the temporal differentiation of activation patterns in left hippocampal dentate gyrus. Thus far, we have shown that LC activation at boundaries relates to later memory separation. Next, we examined whether boundaries decrease the temporal stability of multivoxel activation patterns, an index of pattern separation, in a region highly sensitive to noradrenergic activity: the hippocampal dentate gyrus (DG).

First, we extracted encoding-related multivoxel activation patterns from left and right hippocampal subfields (CA1, CA2/3, and DG) for the two images that would be subsequently queried for temporal memory. These multivoxel patterns were then correlated between each of the to-be-tested item pairmates, providing a trial-level measure of hippocampal subfield pattern similarity. We then compared these pattern similarity measures between boundary-spanning and same-context item pairs using linear mixed modeling analyses for each subfield separately. Our results showed that items spanning an event boundary were associated with lower pattern similarity, or increased pattern separation, in left DG (ß = -.04, p = .017, 95% CI [-0.07, -7.12e-03]; **Figure 3, bottom left**)**.** Importantly, this boundary-induced pattern separation was specific to left DG, as boundaries did not significantly alter pattern similarity in any other subfield (all p's > .05; **Figure 3, bottom left**). Second, we used linear mixed modeling analyses to examine if hippocampal patterns were related to temporal order memory for those same item pairs, and whether those correlations differed by condition. There were no statistically significant main effect or condition-related interaction effects between any hippocampal subfield and temporal order memory (all p's > .05).

Left DG neural differentiation across boundaries corresponds with increased LC BOLD activation. In the next set of linear mixed effects modeling fMRI analyses, we tested another key hypothesis that boundary-induced LC activation promotes neural differentiation in left DG representations, given the critical role of LC-DG pathways in encoding distinct episodic memories (**Figure 3, top panel**). For boundary trials, we found a significant negative correlation between trial-level LC activation and left DG pattern similarity, such that greater LC BOLD activation was related to more dissimilar left DG patterns between item pairs that spanned those same event boundaries (ß = -0.08, p = .0036, 95% CI [-0.13, -0.02], **Figure 3, bottom right**). By contrast, there was a marginally statistically significant positive LC-DG correlation for same-context pairs only (ß = 0.04, p = .085, 95% CI [-5.25e-03, 0.08], **Figure 3, bottom right**).

Importantly, we also found a statistically significant condition-by-LC activation interaction effect, such that LC activation was significantly more correlated with lower pattern similarity in left DG for boundary-spanning pairs compared to same-context pairs (ß = -0.05, p = .002, 95% CI [-0.09, -0.02], **Figure 3, bottom right**). There

were no other significant main, condition-specific, or condition-related interaction effects of tone-evoked LC activation on pattern similarity in any other subfield (all p's > .05). Together, these results demonstrate that phasic increases in LC activation at boundaries relate to greater temporal pattern separation in left DG. Moreover, this functional reconfiguration effect of LC activity was specific to event boundaries and the left DG subfield, suggesting that separation mechanisms are only engaged during behaviorally relevant moments when differentiation is needed.

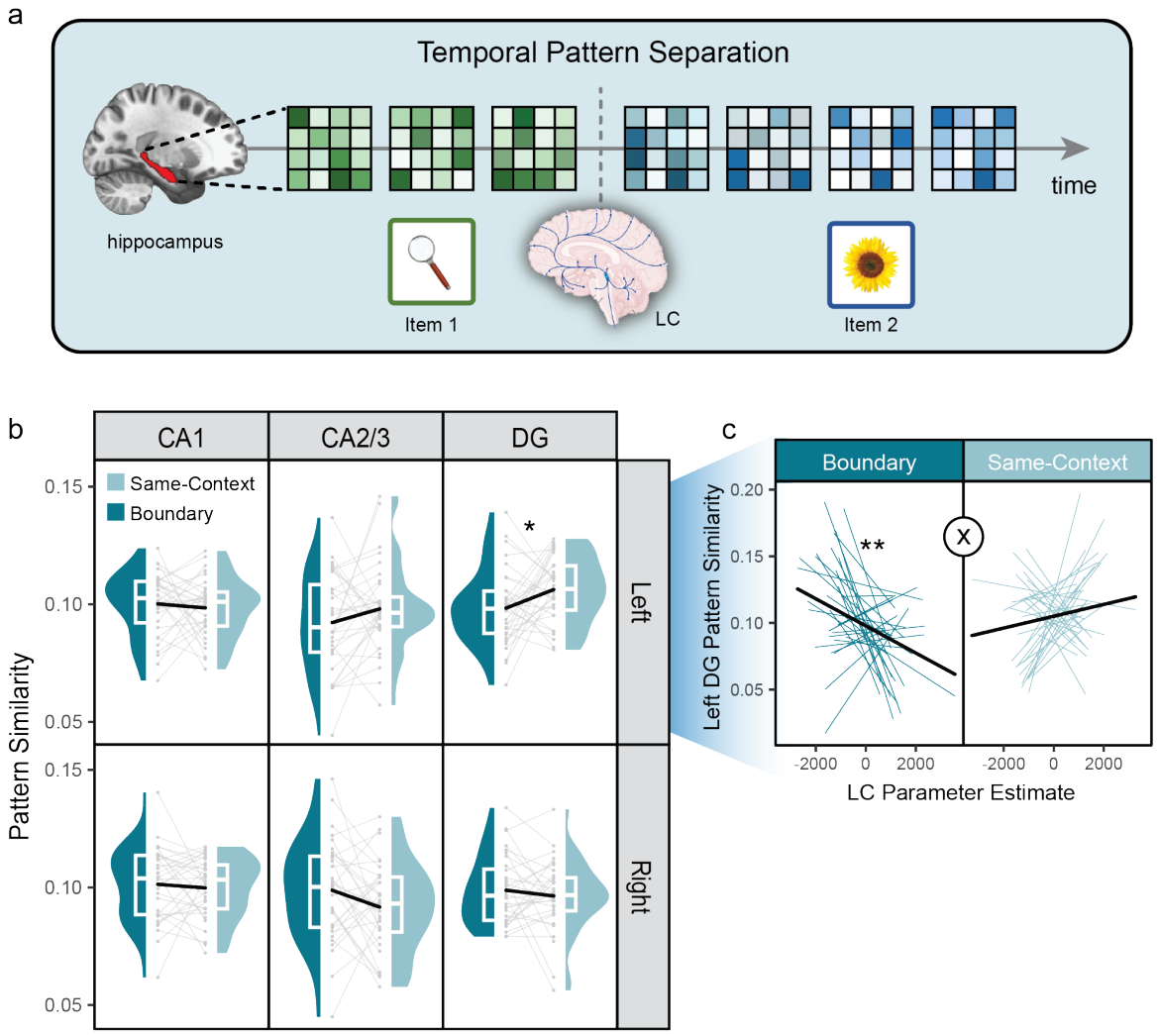

Figure 3. Left dentate gyrus (DG) multivoxel activation patterns were more dissimilar for to-be-tested item pairs that spanned event boundaries, and this neural differentiation effect corresponded with heightened LC activation at those same boundaries. (A) Schematic of key hypothesis that LC activation at event boundaries predicts greater temporal pattern separation in hippocampal DG activation patterns. Colored grids represent multivoxel activation patterns that were extracted from each hippocampal subfield for the to-be-tested item pairs. (B) Boxplots showing differences between hippocampal subfield similarity for boundary pairs versus same-context item pairs during encoding. Colored boxplots represent 25th–75th percentiles of the data, the center line the median, and the error bars the s.e.m. Overlaid dots and connecting grey lines represent data from individual participants ($n = 32$). Note that statistical significance reflects the outcome of linear mixed effects modeling analyses. (C) Linear mixed effects modeling results demonstrating that greater trial-level LC

activation at event boundaries predicts the degree of pattern dissimilarity in left DG specifically, a neural measure of pattern separation. By contrast, intervening LC activation between to-be-tested same-context pairs did not significantly predict left DG pattern similarity for those same item pairs. Individual colored lines represent regression slopes for each participant (n = 32). Dark, bold lines represent the average regression slope across all participants. The "X" symbol represents a statistically significant LC-by-condition interaction effect with p < .01. *p < .05; **p < .001.

Pupillometry Results

Distinct pupil dynamics are sensitive to event boundaries. We have shown previously that context shifts elicit significant increases in pupil dilation, suggesting that boundaries engage central arousal processes[16]. Pupil dilation, however, is complex and is mediated by multiple autonomic pathways and neuromodulatory systems[47,62]. Building on earlier work, we use a temporal principal component analysis (PCA) to decompose boundary-related pupil dilations into its distinct temporal features, providing a unique opportunity to link event segmentation to noradrenergic effects. We also use this PCA approach to examine whether more general pupil-linked arousal mechanisms relate to memory organization and attention.

We first compared average mean pupil dilation responses during tone switches (boundary tones) to mean pupil dilation responses to the repeated tones that occurred within a stable auditory context (i.e., tones preceding items 2-8 within any given 8-item auditory event (**Figure 4A and Figure 4B**). As expected, pupil dilations were indeed significantly greater in response to boundary tones (M = 118.17, SD = 202.38) than to same-context tones (M = 3.04, SD = 182.15; ß = 0.31, p < .001; 95% CI [0.27, 0.35]; **Figure 4A and 4B**).

Next, a temporal PCA was used to decompose average pupil dilation into its constituent temporal features[16]. All pupil samples were averaged across the time-window of tone-evoked pupil dilations (i.e., onset of tone plus 1.5 seconds) and across participants. We selected this limited time-window because it captures the same ISI fixation screen across all tone types and jittered ISI durations. The temporal PCA revealed three canonical pupil components identified in prior work, including a biphasic response that may index separate influences of parasympathetic and sympathetic nervous system regulation on pupil diameter[16,63] (**Figure 4C**)**.** The temporal characteristics of these pupil components, including their latencies-to-peak and percent of explained variance, were as follows: (1) an early-peaking component (684 ms; 89.26% variance); (2) intermediate-peaking component (1,420 ms; 8.40% variance); and (3) a slowly decreasing component (19.6 ms; 1.27% variance).

Using paired t-tests, we found that boundaries significantly modulated loadings, or engagement, of the early-peaking pupil component (component #1; t(27) = 3.63, p = .001, Cohen's d = 0.69; **Figure 4D**) and the intermediate-peaking pupil component (component #2; t(27) = 4.76, p < .001, Cohen's d = 0.90; **Figure 4D**). In contrast, there was no significant effect of event boundaries on loadings for the slowly decreasing pupil component (component #3; t(27) = 0.67, p = .51, Cohen's d = 0.13; **Figure 4D**).

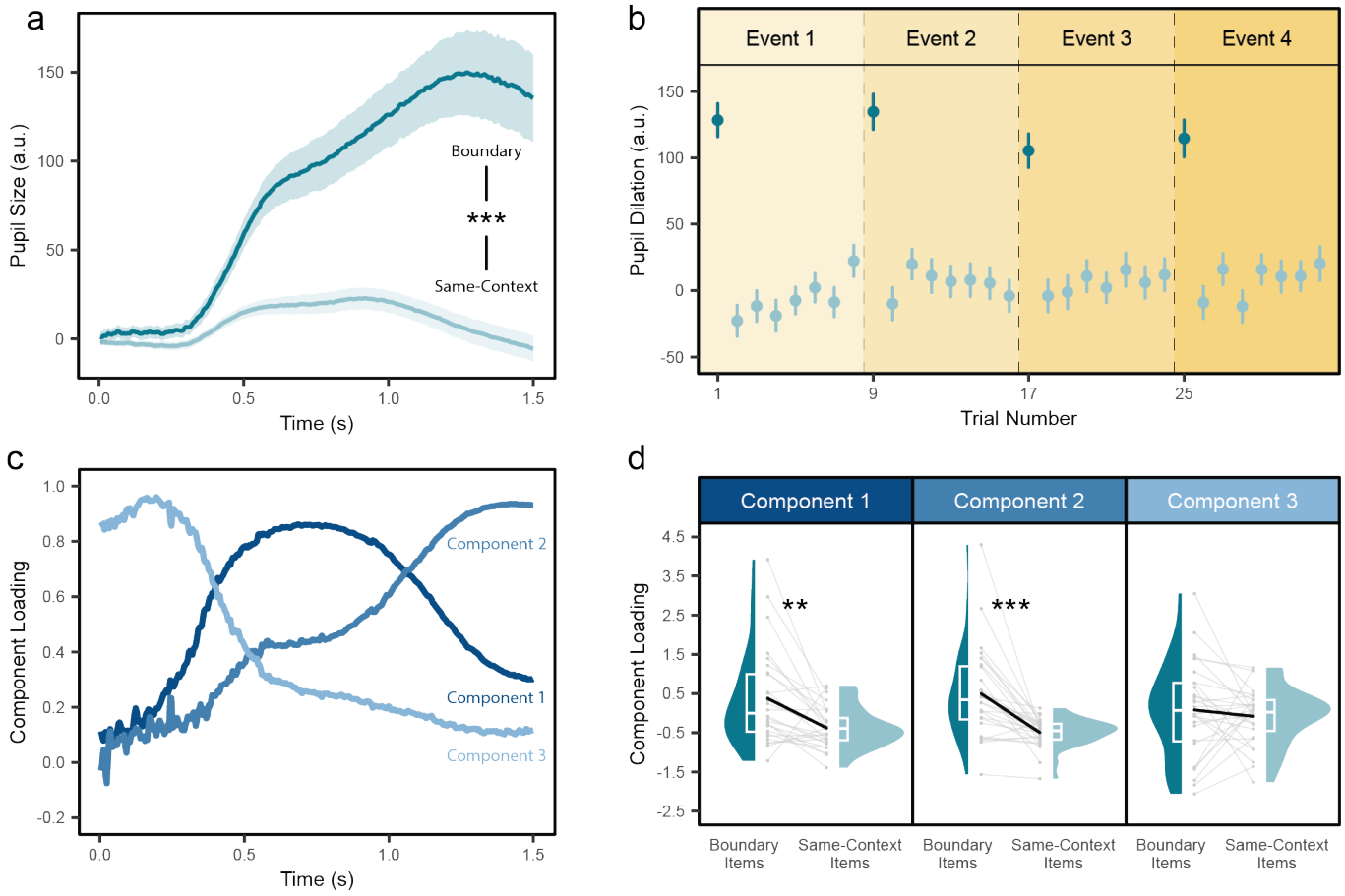

Figure 4. Event boundaries modulate distinct temporal characteristics of the pupil response. (A) Time-course showing the average pupil dilation response evoked by boundary tones (dark green), or tone switches, and same-context, or repeated, tones (light blue). Shaded windows represent s.e.m. at each timepoint. (B) Average pupil dilations plotted as a function of item position within the sequences. Dark blue colors indicate boundary items, or those objects that immediately followed a tone switch. Light blue items indicate objects that immediately followed a same-context, or repeated tone, within a given 8-item auditory event. Vertical bars represent s.e.m. (C) Three temporal features of tone-evoked pupil dilations identified using a temporal principal components analysis (PCA). (D) Statistical comparisons between PCA loadings of the three pupil components between boundary and same-context items. Colored boxplots represent 25th–75th percentiles of the data, the center line the median, and the error bars the s.e.m. Grey dots and connecting lines indicate datapoints from individual participants (n = 28). **p < .01; ***p < .001.

Individual Differences Correlations between Arousal, LC Measures, and Behavior

Using an individual differences approach, we next examined relationships between LC structure/function, attention, and behavioral memory separation. For all measures (except for LC MRI signal intensity), we computed a difference score by subtracting average values for same-context trials from the average values for boundary trials to isolate the specific effects of context shifts. We then correlated these variables across participants using Spearman's rank order correlation analyses.

An early-peaking component of pupil-linked arousal relates to temporal order memory impairments and response-time slowing at boundaries. First, we investigated whether pupil-linked arousal was related to behavioral metrics of event segmentation. We found one statistically significant pupil association with temporal order memory: individuals who showed greater boundary-driven engagement of the early-peaking pupil component also exhibited greater impairments in temporal order memory across boundaries (component #1; ρ = -0.45, p = .017; **Figure 5A**). No other statistically significant pupil-memory associations were observed for the other two pupil components (all p's > .36).

Boundary-driven engagement of this early-peaking pupil component was also positively correlated with greater response time (RT) slowing at boundaries, a potential index of enhanced attention during context shifts (component #1; ρ = 0.38, p = .016; **see Figure 4C for component**). Again, this relationship was only not observed for the other two pupil components (both p's > .05). These results suggest that a specific aspect of pupil dilation, previously implicated in task-relevant responses and parasympathetic nervous system activation[63,64], relates to a disruption in temporal binding processes at boundaries as well as a boost in attention. We furthermore found that boundary-related slowing of response times was correlated with larger boundary-related impairments in temporal order memory (ρ = -0.38, p = .033; **Figure 5A**). Prioritizing local information at event transitions therefore appears to disrupt sequential integration processes[15].

A putative sympathetic nervous system component of pupil-linked arousal relates to LC BOLD activation at boundaries. We next aimed to link a specific sympathetic nervous system-related pupil component, which peaks ~1.5s post-stimulus[64], to phasic increases in LC BOLD activation at boundaries (**see Figure 4C for component)**. Our analyses indeed revealed a significant positive correlation between LC activation evoked by boundaries and loadings on the intermediate-peaking pupil component (component #2; ρ = 0.41, p = .033; **Figure 5A and 5B**). By contrast, LC BOLD responses were not significantly correlated with any other pupil component (both p's > .05). Thus, a distinct temporal feature of stimulus-evoked pupil dilation appears to specifically capture noradrenergic effects, as the LC regulates sympathetic outflow[60].

LC structural integrity relates to diminished boundary-evoked pupil dilations across participants. In a final across-participant correlation analysis, we investigated if a trait-like metric of sustained LC output, neuromelanin MRI signal intensity, relates to changes in arousal and phasic LC activation at boundaries (**Figure 5D**). Spearman's rank order correlations revealed that higher LC signal intensity, or contrast-to-noise ratio (CNR), was negatively correlated with boundary-related loadings on the intermediate-peaking pupil component (component #2; ρ = -0.41, p = .033, **Figure 5A** and **5C; see Figure 4C for component**), consistent with the idea that tonic LC activity blocks task-induced phasic LC activity[65]. LC CNR was not significantly correlated with boundary-related loadings on the other two pupil components (both p's > .05). In contrast to the pupil findings, higher LC CNR was not significantly correlated with boundary-induced LC activation itself (ρ = -0.098, p = 0.59; **Figure 5A**). These findings demonstrate that LC signal intensity is meaningfully related to the pupil dilations elicited by event boundaries, pointing to a potential connection between accumulated patterns of LC output and everyday event perception.

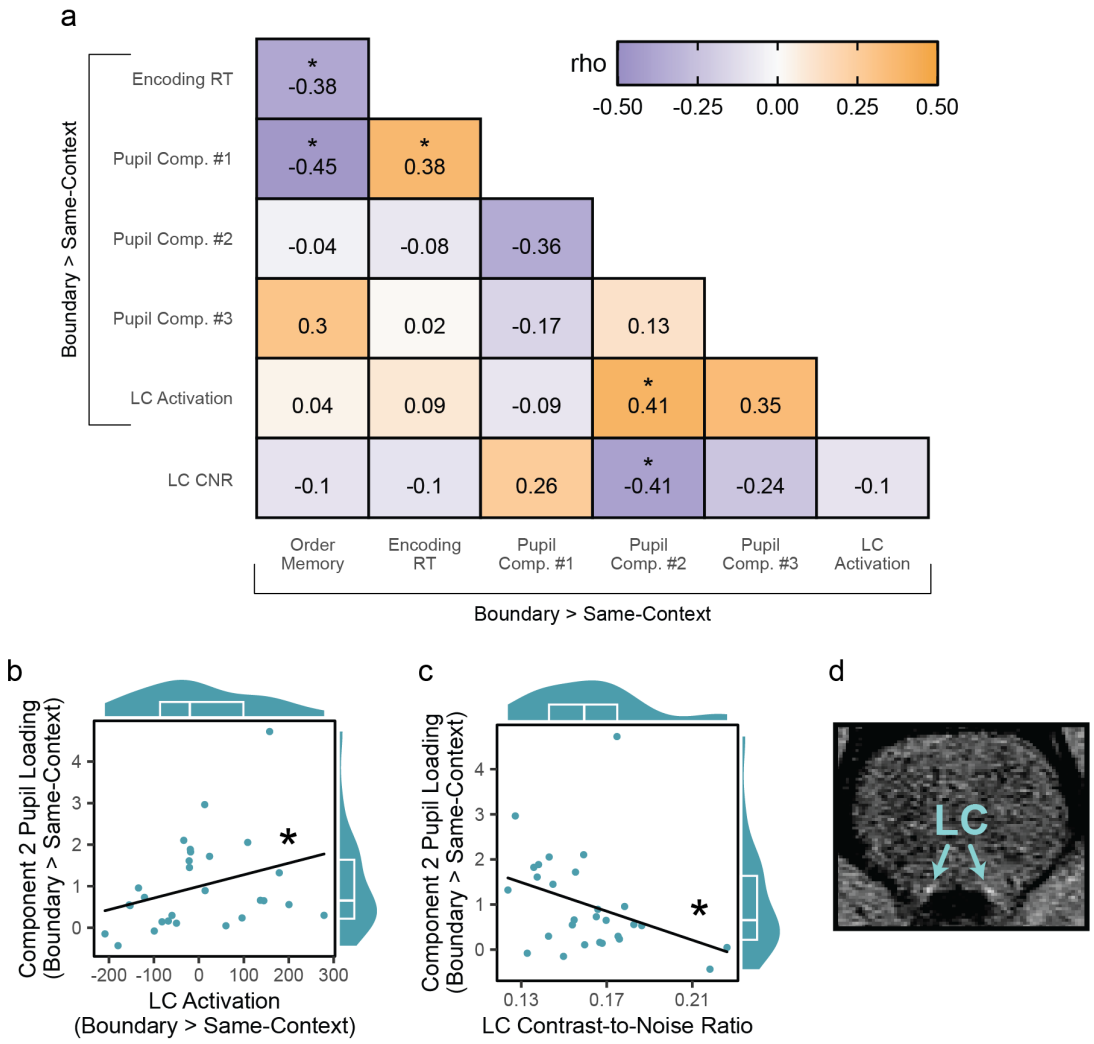

Figure 5. Pupil-linked arousal relates to patterns of LC activation at event boundaries and LC structural integrity. (A) A Spearman's rank order cross-correlation matrix relating key neurophysiological measures of arousal, behavioral metrics of memory separation, and an MRI measure of LC structural integrity across participants. For all functional and behavioral measures, we used subtraction scores of boundary trials versus same-context trials to isolate boundary-specific effects. Pupil variables included loadings from the three aspects of pupil dilation identified by the temporal PCA. Noradrenergic activity was assessed using tone-evoked changes in LC BOLD activation. Behavioral metrics of memory separation included response-time (RT) slowing at boundaries and temporal order memory impairments. LC structure was assessed by extracting the contrast-to-noise ratio (CNR) of LC neuromelanin signal in the fast spin echo images. Within the correlation matrix, colored bar indicates the Spearman's rho correlation coefficient, with purple values indexing negative correlation coefficients and orange boxes indexing positive correlation coefficients. Color saturation reflects the strength of the correlations. (B) A correlation plot showing that higher boundary-induced LC activation was positively correlated with greater boundary-related engagement of pupil dilation component #2. (C) A correlation plot showing that higher LC CNR was associated with smaller boundary-related engagement of pupil dilation component #2. For both correlation plots, marginal density-boxplots depict the median (center line) and interquartile range (25th–75th percentiles) of the x- and y-distributions, and individual dots represent each participants' data. (D) An example participant's neuromelanin MRI image. Bilateral LC nuclei appear as bright dots that standout from their neighboring brainstem tissue and ventricles (arrows). All behavioral and brain correlations have n = 32 participants; any pupil-related correlations have n = 28 participants. *p < .05.

Discussion

The locus coeruleus (LC) is a core hub of the arousal system that facilitates attention and memory[35]. Discrete, momentary bursts of LC activity are critically important for signaling novelty and shifts in environmental contingencies, which could be construed of as 'event boundaries' that punctuate continuous experience. Indeed, prior theories of event segmentation have speculated that catecholamines like dopamine and norepinephrine may trigger segmentation processes in perception and memory[66,67]. However, this hypothesis has never been tested directly.

Here, we provided strong evidence that arousal and LC signaling mediate organizational changes in episodic memory. First, we replicated findings that boundaries segment contextually distinct memories and reliably elicit pupil-linked arousal responses. Importantly, we have now established a critical mechanistic link between boundary-related LC activation and greater behavioral memory separation. We furthermore establish a direct connection between LC responses and hippocampal event representations by showing that LC activation at boundaries relates to greater temporal pattern separation in left dentate gyrus (DG), a hippocampal sub-region known to support encoding and discriminations between highly overlapping inputs. Thus, the noradrenergic system appears to play a critical role in shaping the temporal structure of memory. Finally, using a measure of LC structural integrity, we found that higher LC neuromelanin signal intensity was associated with diminished pupil responses at boundaries, revealing a potential link between a structural metric of chronic LC activation and one's ability to perceive meaningful transitions between events.

Locus coeruleus engagement selectively enhances memory separation at event boundaries

Our key novel finding was that increased LC BOLD activation at boundaries was significantly correlated with reduced temporal order memory across those events, a common behavioral marker of memory separation. This important finding aligns with many influential theories of LC function previously only tested in animal models, including its proposed role in resetting functional brain networks during shifts in environmental contingencies or surprising moments[44,45]. For over a decade, researchers have speculated that catecholamines drive event segmentation processes, largely due to their ability to broadcast prediction errors across the brain and to coordinate attentional and memory processes[66–68]. Using converging methods of pupillometry, fMRI, and behavioral measures of memory separation, we demonstrate that LC engagement during salient context shifts predicts event segmentation effects. Importantly, this LC-memory relationship was specific to boundary trials and was not observed within stable auditory events. LC engagement thereby only influences memory separation during behaviorally relevant moments when internal context representations are rapidly updated and encoded as novel events. If such event model-updating processes were triggered by *any* phasic LC response, memories would potentially become fragmented and organized inappropriately, as they would not align with meaningful environmental changes.

Arousal and locus coeruleus activation mediate the impact of event boundaries on the temporal order memory both within and across individuals

In the present study, event boundaries did not elicit significant increases in LC BOLD signal on average, suggesting that not all context transitions are perceived as equally meaningful and might not warrant later memory separation. One possibility for this null effect is that our boundaries simply were not strong or salient enough to always enlist the LC. Mounting evidence suggests that segmentation processes are heavily determined by task demands and the goal relevance of event boundaries[4,8,10]. As such, simply presenting salient arbitrary stimuli, even if novel, does not necessarily constitute a boundary in long-term memory. For example, simple target detection, which elicits pupil dilation[69], does not relate to temporal order memory impairments used to operationalize event segmentation[70]. Thus, the LC may only drive memory separation when there are meaningful changes in the structure and statistics of the environment that violate an active, stable model of ongoing events[61,71]. This idea is supported by evidence showing that robust pupil dilations only occur during transitions away from a stable, highly patterned sequences of information to a new sequence[72]. It will be important for future studies to identify the factors and conditions under which arousal and LC activation may be enlisted to facilitate event perception and memory.

At the neural level, our results could imply that top-down signals of goal-relevance from other brain regions (e.g., prefrontal cortex) could up-regulate local NE levels in hippocampus at these important moments through a positive feedback loop between glutamate release and NE[34]. The presence of “NE hotspots” could amplify priority signals even further, enhancing processing of the novel sources of information that are needed to update one’s current event model. Likewise, the local release of NE in hippocampus during salient boundaries could also amplify pattern separation processes that began in sensory processing pathways, modulating the outcome of task-related neocortical processes happening upstream[73]. In these ways, LC activity would only enhance encoding of distinct memory representations when it coincides with one’s top-down goals to attend to specific contextual cues and changes.

Our individual difference results furthermore suggest that some individuals may simply be more sensitive to the presence of event boundaries. We found a positive association between boundary-related LC activation and engagement of a specific temporal feature of pupil dilation generally attributed to mental resource allocation[64] and sympathetic nervous system activation[60,64,74]. Multiple neuromodulatory systems, such as the cholinergic and noradrenergic systems, regulate pupil size, making it challenging to dissociate which neuromodulators influence pupil dilation during different cognitive tasks[47,62]. Our results help to establish a specific pupillary signature of LC modulation, enabling pupillometry researchers to specifically infer noradrenergic and SNS activity from this slower-peaking feature of task-induced pupil responses.

Interestingly, boundaries also engaged a pupil response that peaked around 700 milliseconds. Greater boundary-induced engagement of this pupil component was also correlated with impaired order memory and slowed response times at event boundaries, suggesting that it may capture trade-offs between enhanced local boundary processing and temporal encoding processes. Prior work has linked this pupil component to motor and decision-related processes as well as parasympathetic nervous system regulation[60,64]. One possibility is

that it captures contributions from cholinergic activity, as this brain system supports parasympathetic control over pupil dilation[47] as well as enhanced attention and item encoding[75].

Locus coeruleus activation may functionally reconfigure ongoing context representations in left dentate gyrus

Paralleling the effects of LC on behavioral measures of memory, we found that boundaries perturb ongoing contextual representations in the hippocampus, in part through activating the LC. First, using multivoxel pattern similarity analyses, we showed that neural activation patterns in left DG were more differentiated for items with an intervening boundary compared to equidistantly spaced items pairs encountered within the same context. The extent of this DG temporal pattern separation corresponded with greater LC activation across those same boundaries. Like the LC-memory association, this LC-DG effect only occurred for boundary trials and not when the LC was arbitrarily engaged within a stable event.

This functional specificity of LC-DG modulation is highly adaptive because it provides a mechanism by which neural patterns shift during behaviorally relevant moments like boundaries. Consistent with prior frameworks of LC function, LC activation during salient context shifts may directly modulate DG neural patterns to reset ongoing temporal integration processes in hippocampal circuits, leading to the separation of sequential events[39]. Indeed, the LC is densely connected to the DG[37,76,77] and regulates synaptic plasticity in this region[37,38,78]. In rodents, phasic LC activation has been shown to promote global remapping effects in DG, such that novel spatial maps are observed in familiar spatial environments[38,39]. Our findings are consistent with this work, but importantly show that this modulation directly impacts behavioral measures of memory organization in humans. We also build upon animal work by showing that phasic LC activity not only promotes the functional reconfiguration of DG representations for spatial contexts, but also different temporal and perceptual contexts. This LC-mediated reset, in turn, may serve to prioritize and rapidly update mnemonic representations of contextually distinct episodes.

While we did not have an *a priori* hypothesis about laterality, we also found the boundary-related DG pattern separation effect was specific to the left hemisphere. Evidence of strong lateralization effects in hippocampus with respect to memory function is relatively sparse. Interestingly, however, recent work in rodents has shown that context discrimination is higher between spatial environments in the left versus the right DG[79]. Likewise, neuroimaging work in humans has recently linked dynamic patterns of left DG activation to event structure[80]. Future research should investigate the lateralized influences of different hippocampal processes to representing stability and change in the environment.

Chronic LC activation, indirectly indexed by neuromelanin signal, may constrain pupil-related arousal at boundaries, holding important implications for understanding and treating disorders of arousal and memory

Using a combination of pupillometry and neuromelanin MRI, we found that a specific pupil signature of boundaries was correlated with an index of LC structure. Across individuals, both average boundary-evoked pupil dilations and engagement of a sympathetic-related component of pupil dilation were negatively correlated with neuromelanin signal intensity, a putative marker of chronic LC activation. This relationship may reflect the

known trade-offs between tonic and phasic modes of LC activation[65]. Elevated tonic patterns of LC activation, as indirectly evidenced by higher LC signal intensity, may constrain the sensitivity of arousal systems to transient environmental changes, potentially impairing event model updating when it matters.

It is thought that higher LC signal intensity could reflect elevated NE production following prolonged periods of hyperarousal, because the LC help regulate the stress response[81]. Indirect support for this idea comes from studies showing that slow-paced breathing interventions known to quiet sympathetic outflow lead to reductions in LC signal intensity in healthy young adults[59]. Further, it has been shown that LC signal intensity is higher in combat-exposed veterans with PTSD compared to those without PTSD[57] and is correlated with reduced parasympathetic control over the heart[58]. Through this lens, our observation of an association between boundary-induced arousal and a potential noradrenergic marker of stress may have important implications for developing interventions in disorders where disturbances in arousal and memory function intersect. Indeed, deficits in event perception are ubiquitous across disorders marked by aberrant arousal and memory function, including attention deficit hyperactivity disorder[82], Parkinson's disease[83], post-traumatic stress disorder (PTSD)[84–86], and age-related dementia[87].

Insofar as discrete LC responses are needed to signal event boundaries, excessively high levels of arousal and tonic LC activation would likely disrupt normal event segmentation processes. When LC tonic is high, task-relevant phasic LC responses are reduced due to trade-offs between these two modes of activity[65]. But these maladaptive trade-offs could be mitigated, and several strategies could be used to restore "healthier" modes of LC phasic activity to facilitate event cognition and memory. For example, slow-paced breathing[59], vagus nerve stimulation[88], pharmacology[89], and simple exercise[90] have all been shown to enhance LC phasic activity and boost cognitive abilities. Such arousal-related interventions could also be used to augment event segmentation training, a behavioral technique of enhancing the salience of boundaries to improve event detection and enhance long-term memory[91]. Crucially, our findings also highlight a brain system that is likely more accessible for intervention than the hippocampus, which can only engaged indirectly by stimulating cortical regions on the outer surface of the brain[92].

Potential limitations and important considerations for future studies on event segmentation

There are several limitations of the current study that warrant consideration. The LC is notoriously difficult to study in humans due to its small size and its susceptibility to cardiac pulsation artifact in fMRI images[93]. Yet, a rapidly growing neuroimaging literature has provided convincing evidence that LC BOLD signal can be accurately measured and meaningfully linked pupil dilation and/or behavior[50,51,90,94–99]. We used several strategies to mitigate potential issues with studying the LC in humans. First, we used neuromelanin MRI to accurately localize and delineate anatomical masks of the LC in each participant, increasing the spatial specificity of our BOLD measurements. Second, we included physiological nuisance regressors in our fMRI analyses for signal derived from the ventricles, including the fourth ventricle neighboring the LC. These additional variables should have helped control for noise related to cardiac and brainstem pulsation artifacts. Noisy single-trial estimates were also filtered from analyses using a by-participant boxplot outlier detection method, helping reduce any spurious signals driven by physiological artifacts. Third, we did not apply spatial

smoothing to the functional images, helping avoid smearing the BOLD signal beyond the true anatomical boundaries of the LC. While this approach sacrifices some of the signal-to-noise ratio, it also affords better spatial localization of LC-related signal. Fourth, we performed all fMRI analyses in participants' native functional space, avoiding the potential spatial misalignments that can plague group-level LC analyses[100]. Fifth, we used a high-resolution imaging sequence with an in-plane spatial resolution of 1.5mm. This voxel size is sufficient to measure activation in the small LC, which is ~1-3mm wide and ~15mm long[101]. Finally, we corroborated our LC findings using pupillometry, lending additional evidence of a strong connection between phasic LC responses and task-related pupil dilations (for a review, see[46]). Our findings could be further validated using sophisticated imaging tools like cardiac-gated fMRI and 7T fMRI in future work.

Like our functional analyses of the LC, we also did not apply spatial smoothing to our analyses in the hippocampal subfields. It is common to combine the CA23 and DG subfields into a single anatomical mask, given the relatively low spatial resolution of fMRI and small size of these regions. However, we chose to keep these ROIs separate due to substantial evidence that the DG is especially sensitive to fluctuations in noradrenergic activity[37]. It was also evident in our analyses that boundaries led to qualitative differences in CA23 and DG pattern similarity effects. Although not statistically significant, some of these relationships were even in the opposite direction for the two subfields, as with correlations between pattern similarity and temporal order memory. These differences suggest that our ROIs were indeed capturing unique contributions of these subfields to context and memory processing.

An important strength of the current study was the use of a highly controlled and well-validated experimental paradigm to study segmentation effects in memory. This simplicity helped to limit complex interactions with other factors that impact attention and memory function, such as fluctuating task demands, competing contexts, and the semantic relevance of contexts and concurrent memoranda. Nevertheless, many interesting open questions remain about whether the LC is a shared mechanism of event segmentation across multiple contexts and types of event boundaries. For example, recent work suggests that shifts in emotional states can drive memory separation effects and influence temporal memory[102]. However, these segmentation effects were specifically facilitated by changes in emotional valence rather than arousal during sequence encoding, implying limited involvement of the LC. Because emotion was modulated by relatively pleasant musical pieces, it is possible that these boundaries lacked the intense spikes in arousal that may be necessary to engage the LC and impair temporal binding processes in memory. Differences between memory separation and integration might also depend on whether a prediction error-related boundary is signed (i.e., positive or negative) or unsigned (i.e., absolute)[68]. Our basic science findings will be enriched by future investigations using more real-world, naturalistic experiences, which may better capture the complexities of everyday memory function.

Conclusion

In summary, we demonstrate that arousal and noradrenergic modulation help shape the organizational structure of human memory. We also found that the temporal stability of DG representations is perturbed by phasic increases in LC BOLD activation at event boundaries. We propose that this neural separation effect could signify a mental reset of ongoing mental representations, mediated by an LC signal during event

transitions. The LC is responsive to a wide range of behaviorally relevant stimuli, giving it the flexibility to mediate the impact of different types of event boundaries on the structure of memory. We argue, however, that the extent of LC involvement likely depends on the temporal stability of contextual information as well as fluctuations in task engagement and demands for memory separation. By identifying a connection between LC structure and event segmentation, our findings may also provide a neuromechanistic framework for understanding how to study and treat disorders rooted in arousal dysregulation and deficits in episodic memory.

Methods

***Participants*.** Prior to the study, we performed a power analysis to estimate the appropriate sample size using data from a very similar behavioral version of this event boundary experiment[16]. With an alpha = .05 and power = .80, we estimated that we would need 30 participants to obtain a large effect size (d = .80; Cohen's criteria) to achieve enough statistical power to find the weaker of the two memory effects: time dilation effects in temporal distance ratings (G*Power 3.1).

Based on this estimate and to account for potential attrition, a total of 36 healthy young adults were recruited from the New York University (NYU) Psychology Subject Pool and nearby community to participate in this neuroimaging experiment. All participants provided written informed consent approved by the NYU Institutional Review Board and received monetary compensation for their participation. Eligibility criteria included having normal or normal-to-corrected vision and hearing, not taking beta-blockers or other psychoactive drugs, and having no bodily metal to ensure MRI safety.

Data Exclusions. Of those 36 participants, four were excluded from all analyses due to falling asleep in the scanner (n = 3) or due to malfunction of the audio equipment (n = 1). This left a total of thirty-two participants (20 females; $Mean_{age}$ = 22 years old, SD_{age} = 2.7 years) for all behavioral and fMRI analyses. Eleven participants reported being "White", two reported being "Black/African American", 15 reported being "Asian", and 4 reported being "More than one race." For the pupil-related analyses, four additional participants were excluded due to eye-tracker malfunction or poor eye-tracking quality, leaving a subset of twenty-eight participants with valid data for all brain, behavioral, and pupil measurements in this study.

A small subset of participants did not complete all 10 blocks of the event sequence task because they chose to exit the scanner early: two participants completed 7 blocks, one participant had 8 blocks, and one participant had 9 blocks. All remaining data were usable and included in the analyses.

Materials. The object stimuli consisted of 512 color images of everyday objects on a gray background. These images were selected from existing datasets[103,104]. Each image was resized to be 300 x 300 pixels for the encoding phase. For the temporal memory tests, the pair of test images were each resized to be 250 x 250 pixels to create more gaze separation on the screen. The luminance of all object images and fixation screens was normalized using the SHINE toolbox in MATLAB to control for non-cognitive-related effects on pupil size. A total of 320 images were used for encoding, 32 images were used for the practice block outside of the scanner, and 120 images were used as lures in the delayed item recognition test. The practice images were identical across all participants, whereas the encoding and lure items were randomized across participants.

For the auditory context manipulation during sequence encoding, six 1s pure tones with sine waveforms of different frequencies (500Hz, 600Hz, 700Hz, 800Hz, 900Hz, 1000Hz) were generated using Audacity (https://www.audacityteam.org). These frequencies were chosen because they were discriminable from one another and were arousing enough to maintain participants' attention. They were also discriminable from the noise of the scanner.

Overview of Protocol. This study involved one MRI session and one behavioral session ~24 hours later. Upon arriving on Day 1, participants provided written informed consent and completed a demographics form. Next, participants were given instructions about the timeline of scanning and about the event sequence encoding task. They then performed one practice study-test block of the experimental task on a laptop.

Scanning and behavioral procedures. Scanning took approximately 2.5 hours, involving the following sequences in order: one high-resolution anatomical scan, one T2-weighted scan, one neuromelanin MRI scan, and 20 functional scans (10 study rounds interleaved with 10 temporal memory test rounds). Upon entering the MRI scanner, we calibrated the audio equipment while the T2 scan was performed. This audio test ensured that participants could discriminate between the different tone types and could hear the tones comfortably above the noise of the scanner. Participants could adjust tone volume by providing button press feedback to the experimenter. Prior to each encoding list, participants were reminded of the button presses they should use to make their size judgements when viewing each image.

Participants returned to the lab approximately 24 hours later and performed a surprise item recognition memory test. This behavioral session lasted approximately 30 minutes. Given item recognition effects were not central to the hypotheses of the current study, those results are not reported in this manuscript.

Event sequence encoding task. To determine if event boundaries shape the temporal structure of memory, we adapted a behavioral version of a novel paradigm that uses stability and change in auditory contexts to segment memories of neutral image sequences[16] (**Figure 1A**). For each item sequence, participants viewed a series of 32 grayscale, luminance-normed images of objects. Each image was presented in the center of a gray background for 2.5 seconds. A black fixation cross was displayed in the middle of the screen in between each image for 3, 5, or 7 seconds. A 1-s pure tone was played half-way through each jittered ISI in participant's left ear or right ear. This tone indicated to participants which hand they should use to judge if the object was larger or smaller than a standard shoebox (left ear = left hand). To promote associative encoding, participants were also encouraged to link sequential items together by creating a mental narrative.

To create a stable auditory context, or 'event', the specific tone/ear pairing heard before each object remained the same for eight successive objects. After the 8th item in each auditory event, the tone switched to the other ear and changed in pitch, creating a theoretical 'event boundary' in the sequence. This new tone/ear pairing then remained the same for the next eight items, and so on. There were three auditory event boundaries per list, creating a total of four auditory events. Tone frequencies were pseudorandomized across lists such that no tones of a given frequency were presented more than once in a list (e.g., tones that were 700Hz were not heard in more than one event within a given list). Whether the tones first played in participants' left or right ears was counterbalanced across lists. Additionally, 10 separate ISI orders were created, and the order of ISI sequence types across the task was randomized across participants. Each participant viewed a total of 10 lists/sequences in the scanner. Prior to entering the MRI scanner, participants performed one practice study-test block, which familiarized them with the task.

Delay distractor task. To create a 45-s study-test delay and reduce potential recency effects in memory, participants performed an arrow detection task after each sequence. In this phase, a rapid stream of either left-facing (<) or right-facing (>) arrow symbols appeared in the middle of the screen for 0.5s each. Each arrow was separated by a 0.5-s ISI screen with a central fixation cross. Participants simply had to indicate which direction the arrow was pointing via button press as quickly as possible.

Temporal memory tests. Following the distractor task, participants performed two temporal memory tests. On each test trial, different pairs of items from the prior sequence were displayed on the screen for a fixed duration of 8s each. First, participants made a temporal order judgment by indicating which of the two items had appeared more recently during encoding (i.e., "which appeared later?"; **Figure 1**). Participants had four options based on the position of their choice on the screen, which were broken down by confidence: 'definitely left', 'maybe left', 'maybe right', or 'definitely right'. Responses were made using separate button boxes placed in participants' corresponding left and right hands. Participants then made a temporal distance rating in which they endorsed the item pair as having appeared 'very close', 'close', 'far' or 'very far' apart in the prior sequence (i.e., "how far apart?"). The two types of close responses were always made with the left button box and the two types of far responses were always made with the right button box.

Each temporal order and temporal distance test trial was also separated by a slower mini-version of the arrow distractor task, which provided an active baseline for fMRI analyses[105]. During inter-trial-intervals between test trials, a rapid stream of left-facing (<) or right-facing (>) arrow symbols appeared in the middle of the screen for 1s each. Each arrow was separated by a 1-s ISI screen with a central fixation cross. There could be 1, 2 or 3 arrows between each test pair, leading to a jittered temporal interval throughout the memory tests. Critically, each pair of items had always been presented with three intervening items during encoding. They were thereby always encountered the same objective distance apart. Because ISIs during encoding were jittered, we also pseudorandomized the timing of each to-be-tested pair window to always be 32.5s, such that the four ISI's in this behaviorally relevant window summed to 20 seconds.

To test our hypothesis that event boundaries influence the temporal structure of memory, we examined two types of item pairs: (1) items that had appeared within the same auditory event (same-context pairs; 8 trials per list) and (2) items that had spanned an intervening tone switch (boundary-spanning pair; 6 trials per list). The list positions of the to-be-tested pairs were (B = boundary; SC = same-context): 1-5 (SC), 3-7 (SC), 6-10 (B), 8-12 (B), 9-13 (NB), 11-15 (NB), 14-18 (B), 16-20 (B), 17-21 (SC), 19-23 (SC), 22-26 (B), 24-28 (B), 25-29 (SC), and 27-31 (SC).

For all analyses, we removed the first tested item pair from encoding (positions 1 and 5), because it contained the first item in each list and likely constituted a task-irrelevant event boundary. Due to programming errors that were caught partway through the study, for a subset of participants, one block of the task was excluded from all analyses due to the ISI's being 0.5s too short throughout the encoding sequence (n = 9 participants) and one boundary-spanning trial was excluded due to only having two rather than three intervening items (n = 23 participants).

Linear mixed modeling analyses. For all brain, behavioral, and brain-behavior correlation analyses, we performed linear and generalized linear mixed effects modeling analyses in RStudio (version 2022.07.1, R Core Team, 2017) using the *lme4* package (Bates, Maechler, Bolker, & Walker, 2015). Degrees of freedom and p-values were calculated using the *lmerTest* package (Kuznetsova, Brockhoff, & Christensen, 2016). The models were estimated using ML and Nelder-Mead optimizer. Random intercepts for Participant ID (Subject) were modeled as a random effect with a random intercept to control for individual differences. For the temporal order memory logistic regressions, judgments were collapsed across confidence ratings to increase statistical power. Order memory accuracy was then coded as a binary dependent variable (1 = correct, 0 = incorrect). Standardized parameters were obtained by fitting the model on a standardized version of the dataset. 95% Confidence Intervals (CIs) and p-values were computed using a Wald z-distribution approximation.

Eye-Tracking Methods

Eye-tracking. Pupil diameter was measured continuously at 250 Hz during the event sequence task using an infrared EyeLink 1000 eye-tracker system (SR Research, Ontario, Canada). Raw pupil data, segmented by block, were preprocessed using ET-remove-artifacts, a publicly available Matlab program (https://github.com/EmotionCognitionLab/ET-remove-artifacts). This algorithm identifies blinks and other artifacts in the pupil timecourse, then either interpolates over these regions or imputes lengthy periods of artifacts with a missing data indicator (NaN).

Following the approach described in Mathôt et al. (2013)[106], the algorithm detects blink events and other transient artifacts by identifying rapid changes in pupil size, or pupil velocity. The velocity timeseries is computed by applying MATLAB's finite impulse response (FIR) differentiator filter on the raw pupil size timecourse, which provides a robust estimate of instantaneous rate of change while minimizing noise amplification. The parameters for the FIR filter (Filter Order = 14, Passband Frequency = 1, and Stopband Frequency=30) were chosen for this specific dataset (sampled at 250Hz) to ensure distinct and smooth trough-and-peak blink profiles in the velocity timeseries. MATLAB's findpeaks function is then used to identify peaks and troughs in the pupil velocity timecourse. The Peak and Trough Threshold Factor and Trough Threshold Factor, which sets the minimum height constraint to qualify as a peak, were set at 3 or 4 standard deviations of the velocity timeseries, depending on the frequency of blinks for each subject. A contiguous trough followed by a peak in the velocity timeseries was identified as a blink profile.

For artifact removal, linear interpolation is applied across identified blink intervals. Artifact intervals greater than 2 seconds were automatically imputed with NaN (missing data indicator). After applying the algorithm with these settings, a trained user (R.H.) qualitatively inspected the output and occasionally used the ET-Remove-Artifact's Manual Edit functionality. During this process, lengthy periods (>1s) of noisy pupil data were imputed with NaN, and sharp spikes or troughs (<1s in width) missed by the algorithm were interpolated over. A by-participant boxplot outlier approach was used to remove outlier trials from the dataset.

Average boundary-induced pupil dilation analysis. To determine if event boundaries elicit a transient increase in pupil-linked arousal, we compared tone-evoked pupil responses to the boundary tone (i.e., tone

switch after the 8th item in an event) and the same-context, or repeated, tones (i.e., tones that repeated before items 2-8 in a stable auditory event). Tone-evoked pupil dilation was computed as the average pupil diameter 1-1.5s after tone onset minus the average pupil size during the 500ms window prior to tone onset (**Figure 3A**). This time window was chosen because it captured the same post-tone fixation screen shared across all trials and was not confounded by the onset of the ensuing object image. We then performed a linear mixed modeling analysis to test for differences in pupil dilation elicited by boundary versus same-context tones.

Pupil dilation temporal principal component analysis (PCA). A temporal PCA was used to dissociate distinct autonomic and functional components of stimulus-evoked pupil dilations[16]. For each participant and type (boundary tones and same-context tones), we computed the average time-course of baseline-normed pupil dilations across all 1.5-s post-tone time windows. This resulted in 56 input variables (28 participants with one input per condition) to the PCA that contained 375 pupil samples each (see **Figure 3C)**.

An unrestricted PCA using the covariance matrix with Varimax rotation and Kaiser normalization was used to generate meaningful pupil components and component loading scores. These pupil component loadings index temporally dynamic, correlated patterns of pupil dilation elicited by the tones. Factor loadings with eigenvalues greater than 1 were retained and analyzed in subsequent analyses (Kaiser criterion[107]). These PCA loadings reflect the relative degree of engagement of that specific feature of pupil dilation. To determine if boundaries modulated different temporal characteristics of pupil dilation, we performed two-tailed paired t-tests on the loading scores for each pupil component with an alpha = .05 (**Figure 3D**).

fMRI Acquisition and Preprocessing

fMRI/MRI data acquisition. All neuroimaging data were acquired with 3T Siemens Magnetom PRISMA scanner using a 64-channel matrix head coil. Scanning commenced with a high-resolution MPRAGE T1-weighted anatomical scan (slices = 240 sagittal; TR = 2300ms; TE = 2.32 ms; TI = 900 ms; FOV = 230 mm; voxel in-plane resolution = 0.9 mm^2; slice thickness = 0.9 mm; flip angle = 6°; bandwidth = 200 Hz/Px; GRAPPA with acceleration factor = 2; scan duration: 5 min. and 21 s).

This scan was then followed by a T2-weighted scan (slices = 240 sagittal; TR = 3200ms; TE = 564 ms; FOV = 230 mm; voxel in-plane resolution = 0.9 mm^2; slice thickness = 0.9 mm; flip angle = 6°; bandwidth = 200 Hz/Px; GRAPPA with acceleration factor = 2; scan duration: 3 min. and 7 s). During this scan, we also tested and calibrated the audio equipment to ensure the participant could hear the task-related tones above the noise of the scanner. A pair of fieldmap scans were also acquired to aid with functional imaging unwarping, with one scan acquired in the AP phase encoding direction and the other in the PA phase encoding direction. Prior to the encoding task, we collected a neuromelanin MRI scan using a T1-weighted fast spin echo (FSE) imaging sequence (TR = 750 ms; TE = 12ms, voxel in-plane resolution = 0.429 × 0.429 mm^2, slice thickness = 2.5 mm, slice gap = 3.5 mm; flip angle = 120°, 11 axial slices, FOV = 220 mm, bandwidth = 220 Hz/Px).

Separate functional images were collected for each of the interleaved 10 encoding runs and10 retrieval runs of the task. These images were acquired using a single whole-brain T2*-weighted multiband echo planar imaging

(EPI) sequence (128 volumes per encoding run; TR = 2000ms; TE = 28.6 ms, voxel in-plane resolution = 1.5 x 1.5 mm^2; slice thickness = 2 mm with no gap; flip angle = 75°, FOV = 204mm X 204mm; 136 X 136 matrix; phase encoding direction: anterior-posterior; GRAPPA factor = 2; multiband acceleration factor = 2). In each volume, 58 slices were tilted minus 20° of the AC-PC and were collected in an interleaved order.

fMRI preprocessing. Image preprocessing was performed using FSL Version 6.00 (FMRIB's Software Library, www.fmrib.ox.ac.uk/fsl). Functional images were preprocessed using the following steps: removal of non-brain tissue using BET, B0 unwarping using fieldmap images, grand-mean intensity normalization of the 4D data set by a single multiplicative factor, and application of a high-pass temporal filter of 100s. No spatial smoothing was applied to preserve the spatial specificity of anatomical ROI's and to improve pattern similarity estimates[108].

Motion correction was performed using the MCFLIRT tool, resulting in six motion nuisance regressors. Additionally, volumes with extreme head movements, or frame displacements, were labeled and modeled as covariates in the subsequent GLM analyses. Entire blocks with excessive head motion overall (frame displacement > 3mm) were excluded from analysis (across entire dataset = 6 runs). Each participant's denoised mean functional volume were co-registered to their T1-weighted high-resolution anatomical image using brain-based registration (BBR). Anatomical images were then co-registered to the 2mm isotropic MNI-152 standard-space brain using an affine registration with 12 degrees of freedom.

Eight separate physiological nuisance signal regressors were extracted for the subsequent GLM analyses. First, FSL FAST was used to decompose each participant's high-resolution anatomical images into probabilistic tissue masks for white matter (WM), grey matter (GM), and cerebrospinal fluid (CSF). The CSF and WM masks were thresholded at 75% tissue-type probability to increase their spatial specificity and reduce potential overlap. Following a similar approach to Barton et al. (2019)[109], we defined eight 4-mm spheres in representative regions of WM and CSF (four of each type; for exact coordinates, see Barton et al., 2019). Importantly, one of these spheres included a location in the fourth ventricle located adjacent to the locus coeruleus, which helped us mitigate artifact related to cardiac and brainstem pulsation in fMRI scans. The eight spheres and WM and CSF anatomical masks were then transformed into each participant's/run's native functional space and merged to increase their spatial specificity even further. Nuisance timeseries for each of the four WM and four CSF merged masks were then extracted from each run's preprocessed functional data.

Locus Coeruleus and Hippocampal Subfield Region-of-Interest (ROI) Definitions

Locus coeruleus neuromelanin ROI. To acquire participant-specific anatomical LC masks, we collected neuromelanin-weighted MRI scans. LC neurons contain neuromelanin, a byproduct of NE metabolism, thereby enabling its localization via specialized imaging sequences (see **Figure 5D** for example participant's neuromelanin MRI scan). To localize and delineate the LC in each participant, LC ROIs were hand-drawn on each participant's neuromelanin MRI using a similar procedure to a previous study[110]. Bilateral LC anatomical ROIs were manually defined as a three ~1.29 mm wide by ~1.29 mm long masks in three adjacent axial slices where LC signal was brightest and most visible. To identify the most superior slice with the LC, we transformed

a consensus anatomical LC mask from an existing dataset into each participants' neuromelanin image space[111]. The most superior axial slice was defined as highest axial slice that contained this anatomical reference ROI of the LC. For all three axial slices, the LC ROI masks were centered upon the left and right brainstem voxels with the highest MR signal intensities neighboring the corners of the fourth ventricle. We also drew a separate reference mask for the dorsal pontine tegmentum (PT) in each of the three slices, which would later be used to account for overall noise across the images in the neuromelanin signal intensity calculations. This PT reference anatomical ROI was defined as a 10 × 10 voxel square located 6 voxels above the more ventral of the 2 LCs and equidistantly between them.

All masks were hand-drawn by two individuals trained on the anatomy of the LC (R.H. and Z.C.). Their drawings showed high inter-rater reliability (ICC = 0.97). Average LC contrast-to-noise ratio (CNR) was 0.17 and the standard deviation was 0.027, consistent with previously reported CNR values using this fast spin echo MRI sequence (e.g.,[95,110]). For the fMRI and ROI analyses, each participant's neuromelanin MRI image was first brain-extracted using BET and the small field of view parameter (-Z). These brain-extracted neuromelanin scans were then co-registered to each participant's high-resolution anatomical scan using an affine transformation with 6 DOF. We then performed two separate registrations using the inter-space transformation matrices acquired during image preprocessing. Namely, the hand-drawn LC ROIs were first transformed from neuromelanin to anatomical space and then from anatomical space to each participant's run-specific native functional space. All fMRI analyses of the LC were conducted in native functional space.

Hippocampal subfields ROIs. Hippocampal subfields CA2/3, DG, and CA1 were segmented from each participant's high-resolution anatomical scan using Freesurfer 6.0 (https://surfer.nmr.mgh.harvard.edu/). The T2-weighted images were also used to facilitate segmentation. We note that existing fMRI studies tend to use a more conservative approach to segmentation by collapsing DG with CA2/3. However, we opted for a slightly more liberal approach, because we were specifically interested in testing for temporal pattern separation effects in DG[80]. In addition to qualitatively reviewing the subfield segmentation results, the pattern similarity results showed a clear distinction between boundary modulation of CA2/3 and DG. This lends additional support to the idea that the segmentation algorithm was able to successfully distinguish between voxels within these different subfields.

Segmented hippocampal ROIs were co-registered to each participant's native/run-specific functional space for subsequent fMRI pattern similarity analyses. These native-space hippocampal masks were then thresholded at 0.2 to reduce spatial overlap between adjacent subfields. Visual quality checks were performed by the experimenters to ensure anatomical accuracy of these registrations. Each subfield was separated into left and right hemisphere masks based on evidence of potential lateralization of memory processes in hippocampus.

FMRI Analyses

Generalized linear modeling (GLM) analyses and acquisition of single-trial beta estimates. One of the main goals of this study was to test if event boundaries alter responses in the LC and hippocampus, and whether such engagement relates to changes in arousal and how individuals remember the order and timing of recent events. To this end, we first performed Least Squares Separate (LSS) GLM analyses to acquire single-

trial estimates of brain activation, or beta maps, across the whole brain[112,113]. These GLM's were performed on unsmoothed functional data and in each participant's native functional space for each encoding run, separately.

In the LSS procedure, each tone and image from a given sequence was modeled as its own trial-of-interest in separate GLM's, resulting in a unique beta map for each stimulus (n = 64 stimuli per list; 32 tone trials and 32 image trials). Within each single trial GLM, tones were modeled as a stick function with a duration of 1s, while each object image was modeled as a stick function with a duration of 2.5s. The first regressor in each GLM represented the trial of interest (*n* = 1), while the second regressor modeled all other trials (*n* = 63). This modeling process was performed iteratively to generate unique beta maps for each image and tone in the encoding lists. To account for movement artifacts and physiological noise, each GLM included 14 nuisance regressors (4 WM regressors, 4 CSF regressors, and 6 motion regressors). The fsl_motion_outliers tool was also used to identify individual models with extreme head movements. The number of these head movement regressors varied depending on the amount of movement within each run.

Next, we extracted trial-level betas (i.e., parameter estimates) for each tone trial from each participant's LC anatomical mask. Single-trial beta estimates are often noisy due to the transient effects of head motion, cardiac pulsation, and other MRI-related artifacts[108]. To account for potentially spurious estimates of brainstem activation, outlier trials were identified at the participant level using a boxplot outlier removal method. This resulted in the removal of 1.92% of the tone-evoked LC trials from the entire dataset.

Univariate brainstem fMRI analyses. To test if event boundary tones elicited LC activation, we performed linear mixed modeling analyses using the lmer4 package in R. For the logistic regression analysis on temporal order memory, Condition was modeled as a fixed-effect predictor of LC activation (boundary-spanning = 1; same-context = -1). The outlier-cleaned LC responses were mean-centered by participant and then entered as fixed-effects predictors of temporal order memory. Order memory was coded as a binary outcome variable (1 = correct and 0 = incorrect). Subject ID and the side of the screen with the correct answer were modeled as random effects with a random intercepts and constant slopes.

Hippocampal pattern similarity analyses. To test if event boundaries reduce the stability, or similarity, of multivoxel hippocampal representations across time, we performed a multivariate pattern similarity analysis. For each of the six hippocampal subfield ROIs, we first extracted activation patterns from the trial-unique beta maps produced by the LSS GLM (see **Figure 3A** for schematic). Pattern similarity scores were then computed at the item pair level by correlating multivoxel patterns between each of the to-be-tested trial pairs from encoding. For example, we extracted the average multivoxel pattern for images in position 3 and position 7 in each list and then correlated these patterns. This Pearson correlation, or pattern similarity (PS), score provided a neural measure of how similar hippocampal subfield activity patterns were across encoding. As such, lower hippocampal PS values index greater temporal pattern separation, whereas larger PS values index greater pattern integration.

Importantly, the spacing between to-be-tested memory item pairs was large (32.5 seconds) and exceeded the

time course of the canonical hemodynamic response function (HRF). This time window was always identical across all pair types, thereby mitigating potential issues of temporal autocorrelation in the BOLD signal. As before, we used a by-participant boxplot outlier removal method to exclude spurious or noisy PS trials from analysis[108]. This outlier filtering method had a minimal impact on data exclusions, only removing a range of 0.90-1.56% of the PS datapoints across the 6 subfields. The remaining hippocampal PS scores were modeled as outcome variables in a linear mixed effects model, with Condition modeled as a fixed-effect predictor (1 = boundary, -1 = same-context) and Subject modeled as a random effect with a random intercept. To examine if hippocampal pattern stability related to temporal order memory, we performed the same logistic mixed effects modeling analyses as for the LC.

To examine if hippocampal pattern stability relates to transient activation of the LC at event boundaries, we performed additional linear mixed effects models for each subfield, separately. Here, tone-evoked LC parameter estimates were modeled as fixed-effects predictors of hippocampal subfield PS. Condition and its interaction with LC activation were also entered as fixed-effect predictors. Subject ID was modeled as a random effect with a random intercept (see **Figure 3A** for schematic of analyses).

Individual differences correlation analyses

Individual differences analyses were performed between measures of temporal memory (order and distance), pupil-linked arousal, pupil dilation component loadings, encoding response times, LC BOLD activation, and LC neuromelanin signal intensity using Spearman's rank order correlations (see **Figure 5A**). We were specifically interested in isolating boundary-evoked effects on all these neurophysiological and behavioral variables. Thus, for each participant, we computed difference scores by subtracting the average values across all same-context trials from the average values for boundary trials for encoding RT's, pupil loadings from the PCA, mean tone-evoked pupil dilation, and univariate tone-evoked LC BOLD activation. We also computed difference scores for order accuracy by subtracting average performance for all same-context pairs from average values for all boundary-spanning pairs. All these measures were furthermore correlated with neuromelanin contrast-to-noise (CNR) scores to examine their relationship with LC structural integrity.

Data Availability Statement: All behavioral and eye-tracking data will be made available on the Open Science Framework (osf.io/adbm4) upon acceptance of this manuscript.

Code Availability Statement: Code and scripts will be provided on the first author's OSF page (osf.io/adbm4) upon acceptance of this manuscript.

Conflict of Interest Statement: All authors declare no conflicts of interest.

References

1. Zacks, J. M., Speer, N. K., Swallow, K. M., Braver, T. S. & Reynolds, J. R. Event perception: a mind-brain perspective. *Psychological bulletin* **133**, 273 (2007).

2. Radvansky, G. A. Across the event horizon. *Current Directions in Psychological Science* **21**, 269–272 (2012).

3. Clewett, D. & Davachi, L. The ebb and flow of experience determines the temporal structure of memory. *Current Opinion in Behavioral Sciences* **17**, 186–193 (2017).

4. Clewett, D., DuBrow, S. & Davachi, L. Transcending time in the brain: How event memories are constructed from experience. *Hippocampus* **29**, 162–183 (2019).

5. Brunec, I. K., Moscovitch, M. & Barense, M. D. Boundaries Shape Cognitive Representations of Spaces and Events. *Trends in cognitive sciences* (2018).

6. Horner, A. J., Bisby, J. A., Wang, A., Bogus, K. & Burgess, N. The role of spatial boundaries in shaping long-term event representations. *Cognition* **154**, 151–164 (2016).

7. Clewett, D. & McClay, M. Emotional arousal lingers in time to bind discrete episodes in memory. *Cognition and Emotion* No Pagination Specified-No Pagination Specified (2024) doi:10.1080/02699931.2023.2295853.

8. Cowan, E. T., Chanales, A., Davachi, L. & Clewett, D. Goal shifts structure memories and prioritize event-defining information in long- term memory. Preprint at https://doi.org/10.31234/osf.io/ejsrf (2024).

9. Wen, T. & Egner, T. Retrieval context determines whether event boundaries impair or enhance temporal order memory. *Cognition* **225**, 105145 (2022).

10. Wang, Y. C. & Egner, T. Switching task sets creates event boundaries in memory. *Cognition* **221**, 104992 (2022).

11. DuBrow, S. & Davachi, L. The influence of context boundaries on memory for the sequential order of events. *Journal of Experimental Psychology: General* **142**, 1277 (2013).

12. DuBrow, S. & Davachi, L. Temporal memory is shaped by encoding stability and intervening item reactivation. *Journal of Neuroscience* **34**, 13998–14005 (2014).

13. DuBrow, S. & Davachi, L. Temporal binding within and across events. *Neurobiology of learning and memory* **134**, 107–114 (2016).

14. Pu, Y., Kong, X.-Z., Ranganath, C. & Melloni, L. Event boundaries shape temporal organization of memory by resetting temporal context. *Nat Commun* **13**, 622 (2022).

15. Heusser, A. C., Ezzyat, Y., Shiff, I. & Davachi, L. Perceptual boundaries cause mnemonic trade-offs between local boundary processing and across-trial associative binding.

16. Clewett, D., Gasser, C. & Davachi, L. Pupil-linked arousal signals track the temporal organization of events in memory. *Nat Commun* **11**, 4007 (2020).

17. Fortin, N. J., Agster, K. L. & Eichenbaum, H. B. Critical role of the hippocampus in memory for sequences of events. *Nature neuroscience* **5**, 458 (2002).

18. Davachi, L. & DuBrow, S. How the hippocampus preserves order: the role of prediction and context. *Trends in cognitive sciences* **19**, 92–99 (2015).

19. Squire, L. R. Memory and the hippocampus: A synthesis from findings with rats, monkeys, and humans. *Psychological Review* **99**, 195–231 (1992).

20. Howard, M. W. & Eichenbaum, H. The hippocampus, time, and memory across scales. *Journal of Experimental Psychology: General* **142**, 1211 (2013).

21. Tulving, E. & Markowitsch, H. J. Episodic and declarative memory: role of the hippocampus. *Hippocampus* **8**, 198–204 (1998).

22. DuBrow, S., Sherman, B. E., Meager, M. R. & Davachi, L. Medial Temporal Lobe Damage Impairs Temporal Integration in Episodic Memory. *Journal of Cognitive Neuroscience* 1–15 (2024) doi:10.1162/jocn_a_02222.

23. Bakker, A., Kirwan, C. B., Miller, M. & Stark, C. E. L. Pattern separation in the human hippocampal CA3 and dentate gyrus. *Science* **319**, 1640–1642 (2008).

24. Yassa, M. A. & Stark, C. E. L. Pattern separation in the hippocampus. *Trends in neurosciences* **34**, 515–525 (2011).

25. Rolls, E. The mechanisms for pattern completion and pattern separation in the hippocampus. *Frontiers in systems neuroscience* **7**, 74 (2013).

26. O'Reilly, R. C. & McClelland, J. L. Hippocampal conjunctive encoding, storage, and recall: Avoiding a trade-off. *Hippocampus* **4**, 661–682 (1994).

27. Baldassano, C. *et al.* Discovering Event Structure in Continuous Narrative Perception and Memory. *Neuron* **95**, 709-721.e5 (2017).

28. Barnett, A. J. *et al.* Hippocampal-cortical interactions during event boundaries support retention of complex narrative events. *Neuron* **112**, 319-330.e7 (2024).

29. Zheng, J. *et al.* Neurons detect cognitive boundaries to structure episodic memories in humans. *Nat Neurosci* **25**, 358–368 (2022).

30. Michelmann, S. *et al.* Moment-by-moment tracking of naturalistic learning and its underlying hippocampo-cortical interactions. *Nat Commun* **12**, 5394 (2021).

31. Ben-Yakov, A. & Dudai, Y. Constructing realistic engrams: poststimulus activity of hippocampus and dorsal striatum predicts subsequent episodic memory. *Journal of Neuroscience* **31**, 9032–9042 (2011).

32. Ben-Yakov, A., Eshel, N. & Dudai, Y. Hippocampal immediate poststimulus activity in the encoding of consecutive naturalistic episodes. *Journal of Experimental Psychology: General* **142**, 1255 (2013).

33. Berridge, C. W. & Waterhouse, B. D. The locus coeruleus-noradrenergic system: modulation of behavioral state and state-dependent cognitive processes. *Brain Res. Rev.* **42**, 33–84 (2003).

34. Mather, M., Clewett, D., Sakaki, M. & Harley, C. W. Norepinephrine ignites local hot spots of neuronal excitation: how arousal amplifies selectivity in perception and memory. *Behavioral and Brain Sciences* 1–100 (2015).

35. Sara, S. J. The locus coeruleus and noradrenergic modulation of cognition. *Nature Reviews Neuroscience* **10**, 211–223 (2009).

36. Harley, C. W. Norepinephrine in arousal, emotion and learning?: Limbic modulation by norepinephrine and the Kety Hypothesis. *Progress in Neuro-Psychopharmacology & Biological Psychiatry* **11**, 419–458 (1987).

37. Harley, C. W. Norepinephrine and the dentate gyrus. *Dentate Gyrus: A Comphrehensive Guide to Structure, Function, and Clinical Implications* **163**, 299–318 (2007).

38. Grella, S. L. *et al.* Locus Coeruleus Phasic, But Not Tonic, Activation Initiates Global Remapping in a Familiar Environment. *J Neurosci* **39**, 445–455 (2019).

39. Grella, S. L. & Donaldson, T. N. Contextual memory engrams, and the neuromodulatory influence of the locus coeruleus. *Front. Mol. Neurosci.* **17**, (2024).

40. Sara, S. J. Locus Coeruleus in time with the making of memories. *Current opinion in neurobiology* **35**, 87–94 (2015).

41. Sara, S. J. & Segal, M. Plasticity of sensory responses of locus coeruleus neurons in the behaving rat: implications for cognition. *Progress in brain research* **88**, 571–585 (1991).

42. Aston-Jones, G. & Bloom, F. E. Nonrepinephrine-containing locus coeruleus neurons in behaving rats exhibit pronounced responses to non-noxious environmental stimuli. *The Journal of Neuroscience* **1**, 887–900 (1981).

43. Jordan, R. The locus coeruleus as a global model failure system. *Trends in Neurosciences* **47**, 92–105 (2024).

44. Bouret, S. & Sara, S. J. Network reset: a simplified overarching theory of locus coeruleus noradrenaline function. *Trends in Neurosciences* **28**, 574–582 (11AD).

45. Sara, S. J. & Bouret, S. Orienting and reorienting: The locus coeruleus mediates cognition through arousal. *Neuron* **76**, 130–141 (2012).

46. Huang, R. & Clewett, D. The Locus Coeruleus: Where Cognitive and Emotional Processing Meet the Eye. in *Modern Pupillometry: Cognition, Neuroscience, and Practical Applications* (eds. Papesh, M. H. & Goldinger, S. D.) 3–75 (Springer International Publishing, Cham, 2024). doi:10.1007/978-3-031-54896-3_1.

47. Reimer, J. *et al.* Pupil fluctuations track rapid changes in adrenergic and cholinergic activity in cortex. *Nature Communications* **7**, (2016).

48. Joshi, S., Li, Y., Kalwani, R. M. & Gold, J. I. Relationships between pupil diameter and neuronal activity in the locus coeruleus, colliculi, and cingulate cortex. *Neuron* (2015) doi:10.1016/j.neuron.2015.11.028.

49. Varazzani, C., San-Galli, A., Gilardeau, S. & Bouret, S. Noradrenaline and Dopamine Neurons in the Reward/Effort Trade-Off: A Direct Electrophysiological Comparison in Behaving Monkeys. *The Journal of Neuroscience* **35**, 7866–7877 (2015).

50. Murphy, P. R., O'Connell, R. G., O'Sullivan, M., Robertson, I. H. & Balsters, J. H. Pupil diameter covaries with BOLD activity in human locus coeruleus. *Human brain mapping* **35**, 4140–4154 (2014).

51. Lloyd, B., de Voogd, L. D., Mäki-Marttunen, V. & Nieuwenhuis, S. Pupil size reflects activation of subcortical ascending arousal system nuclei during rest. *eLife* **12**, e84822 (2023).

52. Rouhani, N., Norman, K. A., Niv, Y. & Bornstein, A. M. Reward prediction errors create event boundaries in memory. *Cognition* **203**, 104269 (2020).

53. Time for Memories | Journal of Neuroscience. https://www.jneurosci.org/content/43/45/7565.

54. Keren, N. I., Lozar, C. T., Harris, K. C., Morgan, P. S. & Eckert, M. A. In vivo mapping of the human locus coeruleus. *Neuroimage* **47**, 1261–1267 (2009).

55. Keren, N. I. *et al.* Histologic validation of locus coeruleus MRI contrast in post-mortem tissue. *NeuroImage* **113**, 235–245 (2015).

56. Sasaki, M. *et al.* Neuromelanin magnetic resonance imaging of locus ceruleus and substantia nigra in Parkinson's disease. *Neuroreport* **17**, 1215–1218 (2006).

57. McCall, A. *et al.* Evidence for locus coeruleus-norepinephrine system abnormality in military PTSD revealed by neuromelanin-sensitive MRI. *Biological Psychiatry* (2024) doi:10.1016/j.biopsych.2024.01.013.

58. Mather, M. *et al.* Higher locus coeruleus MRI contrast is associated with lower parasympathetic influence over heart rate variability. *NeuroImage* **150**, 329–335 (2017).

59. Bachman, S. L. *et al.* Daily heart rate variability biofeedback training decreases locus coeruleus MRI contrast in younger adults. 2022.02.04.22270468 Preprint at https://doi.org/10.1101/2022.02.04.22270468 (2022).

60. Loewenfeld, I. E. & Lowenstein, O. *The Pupil: Anatomy, Physiology, and Clinical Applications*. vol. 2 (Wiley-Blackwell, 1993).

61. Rouhani, N., Clewett, D. & Antony, J. W. Building and Breaking the Chain: A Model of Reward Prediction Error Integration and Segmentation of Memory. *Journal of Cognitive Neuroscience* 1–13 (2024) doi:10.1162/jocn_a_02215.

62. Larsen, R. S. & Waters, J. Neuromodulatory correlates of pupil dilation. *Frontiers in neural circuits* **12**, 21 (2018).

63. Steinhauer, S. R. & Hakerem, G. The pupillary response in cognitive psychophysiology and schizophrenia. *Annals of the New York Academy of Sciences* **658**, 182–204 (1992).

64. Steinhauer, S. R., Siegle, G. J., Condray, R. & Pless, M. Sympathetic and parasympathetic innervation of pupillary dilation during sustained processing. *International journal of psychophysiology* **52**, 77–86 (2004).

65. Aston-Jones, G. & Cohen, J. D. An integrative theory of locus coeruleus-norepinephrine function: Adaptive gain and optimal performance. *Annual Review of Neuroscience* **28**, 403–450 (2005).

66. Zacks, J. M. & Sargent, J. Q. Event perception: A theory and its application to clinical neuroscience. *Psychology of learning and motivation* **53**, 253–299 (2010).

67. Zacks, J. M., Kurby, C. A., Eisenberg, M. L. & Haroutunian, N. Prediction error associated with the perceptual segmentation of naturalistic events. *Journal of Cognitive Neuroscience* **23**, 4057–4066 (2011).

68. Rouhani, N., Niv, Y., Frank, M. J. & Schwabe, L. Multiple routes to enhanced memory for emotionally relevant events. *Trends in Cognitive Sciences* **27**, 867–882 (2023).

69. Swallow, K. M., Jiang, Y. V. & Riley, E. B. Target detection increases pupil diameter and enhances memory for background scenes during multi-tasking. *Sci Rep* **9**, 5255 (2019).

70. Wang, Y. C. & Egner, T. Target detection does not influence temporal memory. *Atten Percept Psychophys* **85**, 1936–1948 (2023).

71. Siefke, B. M., Smith, T. A. & Sederberg, P. B. A context-change account of temporal distinctiveness. *Memory & cognition* 1–15 (2019).

72. Zhao, S. *et al.* Pupil-linked phasic arousal evoked by violation but not emergence of regularity within rapid sound sequences. *Nature communications* **10**, (2019).

73. Amer, T. & Davachi, L. Extra-hippocampal contributions to pattern separation. *eLife* **12**, e82250 (2023).

74. Widmann, A., Schröger, E. & Wetzel, N. Emotion lies in the eye of the listener: Emotional arousal to novel sounds is reflected in the sympathetic contribution to the pupil dilation response and the P3. *Biological psychology* **133**, 10–17 (2018).

75. Hasselmo, M. E. The Role of Acetylcholine in Learning and Memory. *Curr Opin Neurobiol* **16**, 710–715 (2006).

76. Loy, R., Koziell, D. A., Lindsey, J. D. & Moore, R. Y. Noradrenergic innervation of the adult rat hippocampal formation. *Journal of Comparative Neurology* **189**, 699–710 (1980).

77. Blackstad, T. W., Fuxe, K. & Hökfelt, T. Noradrenaline nerve terminals in the hippocampal region of the rat and the guinea pig. *Z Zellforsch Mikrosk Anat* **78**, 463–473 (1967).

78. Walling, S. G. & Harley, C. W. Locus ceruleus activation initiates delayed synaptic potentiation of perforant path input to the dentate gyrus in awake rats: A novel beta-adrenergic- and protein synthesis-dependent mammalian plasticity mechanism. *Journal of Neuroscience* **24**, 598–604 (2004).

79. Cholvin, T. & Bartos, M. Hemisphere-specific spatial representation by hippocampal granule cells. *Nat Commun* **13**, 6227 (2022).

80. Bein, O. & Davachi, L. Event Integration and Temporal Differentiation: How Hierarchical Knowledge Emerges in Hippocampal Subfields through Learning. *J. Neurosci.* **44**, e0627232023 (2024).

81. Berridge, C. W. Noradrenergic modulation of arousal. *Brain Research Reviews* **58**, 1–17 (2008).

82. Event Segmentation Deficits in ADHD - Julia Ryan, Maria Rogers, 2021. https://journals.sagepub.com/doi/10.1177/1087054718799929?url_ver=Z39.88-2003&rfr_id=ori:rid:crossref.org&rfr_dat=cr_pub%20%200pubmed.

83. Wyrobnik, M., van der Meer, E. & Klostermann, F. Relation between event segmentation and memory dysfunction in Parkinson's disease. *Brain and Cognition* **163**, 105912 (2022).

84. Pitts, B. L., Eisenberg, M. L., Bailey, H. R. & Zacks, J. M. Cueing natural event boundaries improves memory in people with post-traumatic stress disorder. *Cogn Res Princ Implic* **8**, 26 (2023).

85. Pitts, B. L., Eisenberg, M. L., Bailey, H. R. & Zacks, J. M. PTSD is associated with impaired event processing and memory for everyday events. *Cognitive Research: Principles and Implications* **7**, 35 (2022).

86. Eisenberg, M. L., Sargent, J. Q. & Zacks, J. M. Posttraumatic Stress and the Comprehension of Everyday Activity. *Collabra* **2**, 11 (2016).

87. Zacks, J. M., Speer, N. K., Vettel, J. M. & Jacoby, L. L. Event understanding and memory in healthy aging and dementia of the Alzheimer type. *Psychology and aging* **21**, 466 (2006).

88. Hulsey, D. R. *et al.* Parametric characterization of neural activity in the locus coeruleus in response to vagus nerve stimulation. *Exp Neurol* **289**, 21–30 (2017).

89. Levey, A. I. *et al.* A phase II study repurposing atomoxetine for neuroprotection in mild cognitive impairment. *Brain* **145**, 1924–1938 (2022).

90. Mather, M. *et al. Isometric Exercise Facilitates Attention to Salient Events in Women via the Noradrenergic System*. http://biorxiv.org/lookup/doi/10.1101/749002 (2019) doi:10.1101/749002.

91. Gold, D. A., Zacks, J. M. & Flores, S. Effects of cues to event segmentation on subsequent memory. *Cognitive Research: Principles and Implications* **2**, 1 (2017).

92. Hermiller, M. S. *et al.* Evidence from theta-burst stimulation that age-related de-differentiation of the hippocampal network is functional for episodic memory. *Neurobiol Aging* **109**, 145–157 (2022).

93. Astafiev, S. V., Snyder, A. Z., Shulman, G. L. & Corbetta, M. Comment on “Modafinil shifts human locus coeruleus to low-tonic, high-phasic activity during functional MRI” and “Homeostatic sleep pressure and responses to sustained attention in the suprachiasmatic area”. *Science* **328**, 309–309 (2010).

94. Jacobs, H. I. *et al.* Dynamic behavior of the locus coeruleus during arousal-related memory processing in a multi-modal 7T fMRI paradigm. *eLife* **9**, e52059 (2020).

95. Clewett, D., Huang, R., Velasco, R., Lee, T.-H. & Mather, M. Locus coeruleus activity strengthens prioritized memories under arousal. *Journal of Neuroscience* 2097–17 (2018).

96. Clewett, D., Schoeke, A. & Mather, M. Locus coeruleus neuromodulation of memories encoded during negative or unexpected action outcomes. *Neurobiology of Learning and Memory* **111**, 65–70 (5AD).

97. Minzenberg, M. J., Watrous, A. J., Yoon, J. H., Ursu, S. & Carter, C. S. Modafinil shifts human locus coeruleus to low-tonic, high-phasic activity during functional MRI. *Science* **322**, 1700–1702 (2008).

98. Köhler, S., Bär, K. & Wagner, G. Differential involvement of brainstem noradrenergic and midbrain dopaminergic nuclei in cognitive control. *Human brain mapping* **37**, 2305–2318 (2016).

99. Liu, K. Y. *et al.* Magnetic resonance imaging of the human locus coeruleus: A systematic review. *Neuroscience & Biobehavioral Reviews* **83**, 325–355 (2017).

100. Yi, Y.-J. *et al.* It is the locus coeruleus! Or… is it?: a proposition for analyses and reporting standards for structural and functional magnetic resonance imaging of the noradrenergic locus coeruleus. *Neurobiology of Aging* **129**, 137–148 (2023).

101. Fernandes, P., Regala, J., Correia, F. & Gonçalves-Ferreira, A. J. The human locus coeruleus 3-D stereotactic anatomy. *Surg Radiol Anat* **34**, 879–885 (2012).

102. McClay, M., Sachs, M. E. & Clewett, D. Dynamic emotional states shape the episodic structure of memory. *Nat Commun* **14**, 6533 (2023).

103. Gabrieli, J. D. E., Brewer, J. B., Desmond, J. E. & Glover, G. H. Seperate neural bases of two fundamental memory processes in the human medial temporal lobe. *Science* **276**, 264–266 (1997).

104. Kensinger, E. A., Garoff-Eaton, R. J. & Schacter, D. L. Memory for specific visual details can be enhanced by negative arousing content. *Journal of Memory and Language* **54**, 99–112 (2006).

105. Stark, C. E. L. & Squire, L. R. When zero is not zero: The problem of ambiguous baseline conditions in fMRI. *Proceedings of the National Academy of Sciences of the United States of America* **98**, 12760–12765 (2001).

106. Mathôt, S. A simple way to reconstruct pupil size during eye blinks. in 0 Bytes (figshare, 2013). doi:10.6084/M9.FIGSHARE.688001.V1.

107. Kaiser, H. F. The application of electronic computers to factor analysis. *Educational and psychological measurement* **20**, 141–151 (1960).

108. Dimsdale-Zucker, H. R. & Ranganath, C. Chapter 27 - Representational Similarity Analyses: A Practical Guide for Functional MRI Applications. in *Handbook of Behavioral Neuroscience* (ed. Manahan-Vaughan, D.) vol. 28 509–525 (Elsevier, 2018).

109. Bartoň, M. *et al.* Evaluation of different cerebrospinal fluid and white matter fMRI filtering strategies—Quantifying noise removal and neural signal preservation. *Hum Brain Mapp* **40**, 1114–1138 (2018).

110. Clewett, D. *et al.* Neuromelanin marks the spot: Identifying a locus coeruleus biomarker of cognitive reserve in healthy aging. *Neurobiology of Aging* **37**, 117–126 (2016).

111. Dahl, M. J. *et al.* Locus coeruleus integrity is related to tau burden and memory loss in autosomal-dominant Alzheimer's disease. *Neurobiology of Aging* **112**, 39–54 (2022).

112. Mumford, J. A., Davis, T. & Poldrack, R. A. The impact of study design on pattern estimation for single-trial multivariate pattern analysis. *Neuroimage* **103**, 130–138 (2014).

113. Mumford, J. A., Turner, B. O., Ashby, F. G. & Poldrack, R. A. Deconvolving BOLD activation in event-related designs for multivoxel pattern classification analyses. *Neuroimage* **59**, 2636–2643 (2012).